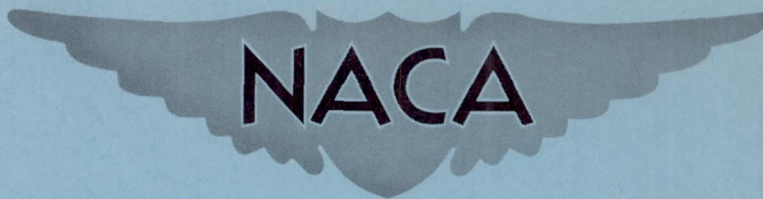


NACA RM L51D20



# RESEARCH MEMORANDUM

LOW-SPEED INVESTIGATION OF SEVERAL TYPES OF SPLIT FLAP  
ON A 47.7° SWEPTBACK-WING - FUSELAGE COMBINATION OF  
ASPECT RATIO 5.1 AT A REYNOLDS NUMBER OF  $6.0 \times 10^6$

By Stanley H. Spooner and Ernst F. Mollenberg

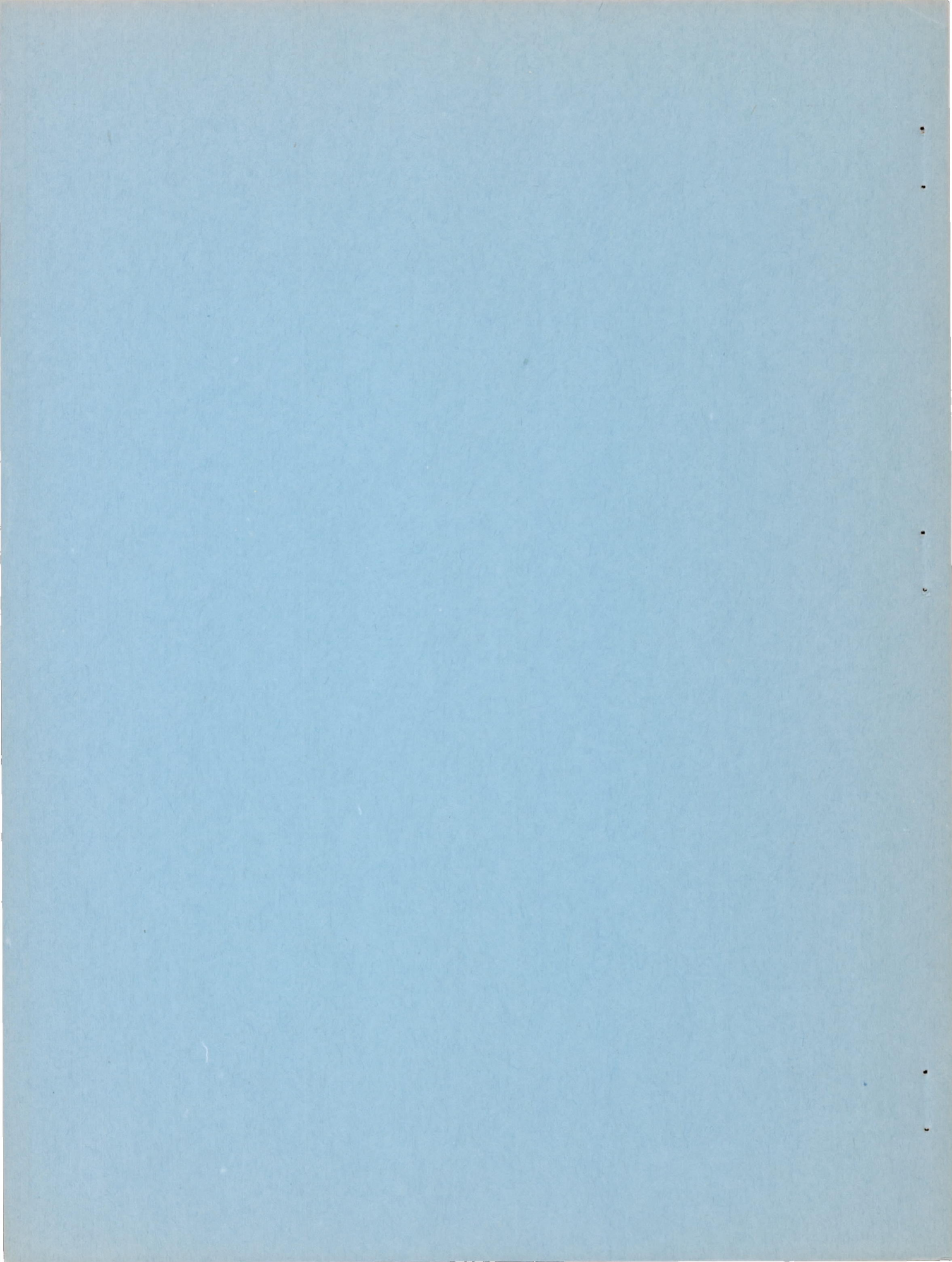
Langley Aeronautical Laboratory  
Langley Field, Va.

NATIONAL ADVISORY COMMITTEE  
FOR AERONAUTICS

WASHINGTON

July 10, 1951





## NATIONAL ADVISORY COMMITTEE FOR AERONAUTICS

## RESEARCH MEMORANDUM

## LOW-SPEED INVESTIGATION OF SEVERAL TYPES OF SPLIT FLAP

ON A  $47.7^\circ$  SWEEPBACK-WING - FUSELAGE COMBINATION OF  
ASPECT RATIO 5.1 AT A REYNOLDS NUMBER OF  $6.0 \times 10^6$

By Stanley H. Spooner and Ernst F. Mollenberg

## SUMMARY

A low-speed wind-tunnel investigation has been conducted at a Reynolds number of  $6.0 \times 10^6$  to determine the longitudinal aerodynamic characteristics of a  $47.7^\circ$  sweptback-wing - fuselage combination equipped with split flaps and various modifications thereof. The modifications consisted of extended split (Zap), rotated split, step split, and triangular flaps. The wing had an aspect ratio of 5.1, a taper ratio of 0.383, and NACA 64-210 airfoil sections normal to the 0.286-chord line. The maximum wing thickness in a streamwise direction was 7.5 percent of the wing chord.

The largest values of maximum lift coefficient  $C_{L_{\max}}$  and increment of lift coefficient were obtained with deflection angles of the order of  $40^\circ$  with those flaps having hinge lines located on or near the wing trailing edge and compare favorably with the values obtained with double slotted flaps of the same span. When the wing is equipped with leading-edge flaps, the longitudinal stability in the high-lift range below  $C_{L_{\max}}$  is dependent upon the type of trailing-edge flap and the degree of deflection.

Maximum lift coefficients up to 1.65 were obtained with extended split-flap configurations having stable pitching-moment characteristics at  $C_{L_{\max}}$ .



## INTRODUCTION

As part of an investigation to supply additional information concerning the effectiveness of various types of flaps on wings having sweptback plan forms, together with the effects of flap deflection, span, and chordwise position, the effectiveness of various types of flap has been evaluated on a  $47.7^\circ$  sweptback-wing - fuselage combination. Reference 1 presents the results obtained from tests of single slotted flaps. The present paper reports the results of tests of flaps of the split type.

The tests were conducted in the Langley 19-foot pressure tunnel at a Reynolds number of  $6.0 \times 10^6$  and a Mach number of 0.14. The wing had an aspect ratio of 5.1, a taper ratio of 0.383, and NACA 64-210 airfoil sections normal to the 0.286-chord line. For most of the tests a fuselage was attached to the wing. The flaps investigated were split, extended split (Zap), rotated split, step split, and triangular, and were tested in combination with several spans of leading-edge flap.

## NOTATION

The data are referred to a set of axes coinciding with the wind axes and originating in the plane of symmetry at the quarter-chord point of the mean aerodynamic chord. All wing coefficients are based upon the dimensions of the basic wing.

$C_L$  lift coefficient (Lift/ $qS$ )

$C_{L_{max}}$  maximum lift coefficient

$\Delta C_L$  increment of lift coefficient due to flap deflection, measured at  $\alpha = 8^\circ$

$C_D$  drag coefficient (Drag/ $qS$ )

$C_m$  pitching-moment coefficient (Pitching moment/ $qS\bar{c}$ )

$q$  free-stream dynamic pressure, pounds per square foot

$S$  wing area, square feet



$\bar{c}$	mean aerodynamic chord, feet $\left(\frac{2}{S} \int_0^{b/2} c^2 dy\right)$
$c$	wing chord, parallel to plane of symmetry, feet
$c'$	wing chord normal to 0.286c, feet
$b/2$	semispan of wing, normal to plane of symmetry, feet
$y$	spanwise coordinate, normal to plane of symmetry, feet
$L/D$	ratio of lift to drag
$R$	Reynolds number, based on mean aerodynamic chord
$\delta_f$	flap deflection, degrees
$\alpha$	angle of attack of root chord, degrees
$\Lambda$	angle of sweepback of the 0.286c line, degrees
$\theta$	angle of glide, degrees $(\cot^{-1} L/D)$
$V_g$	gliding speed, miles per hour
$V_v$	sinking speed, feet per second

## MODEL

The principal dimensions of the model are shown in figure 1. The wing, which was of solid-steel construction, had NACA 64-210 airfoil sections normal to the 0.286-chord line. The sweepback of the 0.286-chord line (0.25c') was  $45^\circ$ , the aspect ratio was 5.1, and the taper ratio was 0.383. The maximum wing thickness in a plane parallel to the plane of symmetry was 0.075c. The wing was uniformly twisted to produce  $1.32^\circ$  washout at the tip and the dihedral angle was  $0^\circ$ . The wing was located on the fuselage in a midwing position and at  $2^\circ$  incidence with respect to the fuselage center line. The fuselage was of circular cross section and had a fineness ratio of 10.2.

The geometric characteristics of the leading-edge flaps and the trailing-edge flaps are shown in figures 1 and 2, respectively. All flaps were fabricated from either steel or aluminum sheet and the

brackets were of steel. The leading-edge flaps had a constant chord of 0.098c and a deflection of  $45^\circ$ . The outboard end was fixed at station  $0.975b/2$  for the several spans tested.

The trailing-edge split flaps had a constant percent chord of  $0.20c'$  and could be deflected  $15^\circ$ ,  $30^\circ$ ,  $45^\circ$ , and  $60^\circ$ . With the fuselage attached to the wing, the flap sections inboard of station  $0.144b/2$  were removed.

The extended split and rotated split flaps were so designed that when they extended from the plane of symmetry to the  $0.50b/2$  station the areas were equal to the area of the split flap of the same span and spanwise location. The step split flaps were equal in area to the split flaps which extended from  $0.144b/2$  to  $0.45b/2$ . The triangular flaps, when tested with the wing-fuselage combination, had trailing edges normal to the plane of symmetry in the deflected position and an area equal to that of the split flaps which extended from  $0.144b/2$  to  $0.45b/2$ . The triangular flaps, when tested on the wing alone, were geometrically similar to the triangular flaps described above but were equal in area to the split flaps extending from the plane of symmetry to the  $0.50b/2$  station. With the exception of the triangular flaps, the flap plan forms were tapered in a manner such that extensions of the leading and trailing edge of each flap would intersect at the same distance from the plane of symmetry.

The separator plate used with some of the tests of the step split flaps consisted of a plate parallel to the plane of symmetry extending from the outboard end of the inboard step to the inboard end of the outboard step.

A photograph of the model mounted in the Langley 19-foot pressure tunnel is presented as figure 3.

#### TESTS

The tests were conducted in the Langley 19-foot pressure tunnel with the air compressed to approximately 33 pounds per square inch, absolute. The tests were made at a Reynolds number of  $6.0 \times 10^6$  and a Mach number of 0.14.

The lift, drag, and pitching moments were measured through an angle-of-attack range at zero yaw by a simultaneously recording balance system. The characteristics of the wing and the wing-fuselage were determined for numerous combinations of leading-edge-flap span and trailing-edge-flap type, span, and deflection.



## RESULTS AND DISCUSSION

All data have been reduced to standard nondimensional coefficients and have been corrected for support tare and interference effects and for air-stream misalignment. Jet-boundary corrections have been applied to the angle of attack and to the drag and pitching-moment coefficients. The jet-boundary induced velocities obtained by means of reference 2 were used to compute these corrections.

The extensive number of flap configurations investigated prevents the inclusion in this paper of all the data obtained in the tests. The data are presented in figures 4 to 16 for those configurations considered to be the most promising of each flap type and for those configurations necessary to show the effects of the several variables. The pertinent data for the remaining configurations are presented in tables I and II.

## Lift Characteristics

Maximum lift.- The highest values of maximum lift coefficient measured for the wing-fuselage combination are obtained with the extended split flaps in combination with the leading-edge flaps. As shown in table I, these values are 1.57 and 1.70 for flap spans of  $0.45b/2$  and  $0.60b/2$ , respectively. The maximum values of  $C_{L_{max}}$  for the split flap configurations are 1.50 and 1.59. With the exception of the forward-located step flaps, the other flaps tested produce values of  $C_{L_{max}}$  about the same as those of the split flaps. The forward-located step flaps produce a  $C_{L_{max}}$  about 0.15 less.

Some examples of the effects of flap deflection and span on the lift characteristics are shown in figures 4 and 5 for the split and extended split flaps. The variation of  $C_{L_{max}}$  with flap deflection is shown in figure 17. With the  $0.425b/2$  leading-edge flaps and the  $0.45b/2$  split flaps, a maximum value of  $C_{L_{max}}$  of 1.45 is obtained at  $\delta_f = 30^\circ$ . For deflections greater than  $\delta_f = 30^\circ$ , the value of  $C_{L_{max}}$  decreases until at  $\delta_f = 60^\circ$   $C_{L_{max}}$  is 1.34. The  $0.60b/2$  split flaps give a similar variation of  $C_{L_{max}}$  with deflection. Table I indicates that  $C_{L_{max}}$  of the configuration with undeflected trailing-edge flaps was not necessarily reached. For the deflection range investigated the variation of  $C_{L_{max}}$  with  $\delta_f$  may, therefore, be even less than that

shown. For the extended split flaps the maximum values of  $C_{L_{max}}$  occur at slightly higher deflections, about  $45^\circ$ . Table I shows that, regardless of the leading-edge flap span, the maximum values of  $C_{L_{max}}$  are obtained at deflections of approximately  $30^\circ$  and  $45^\circ$ , respectively, for the split and extended split flaps.

Examples of the effects of leading-edge flap span on the lift characteristics are shown in figures 6 and 7. The variation of  $C_{L_{max}}$  with span of the leading-edge flaps is shown in figure 18 for the wing-fuselage combination equipped with and without the split and extended split flaps. With the split flaps the highest values of  $C_{L_{max}}$  are attained with the inboard end of the leading-edge flaps extending to between the  $0.55b/2$  and  $0.45b/2$  stations. For the configuration of the extended split flaps deflected  $30^\circ$   $C_{L_{max}}$  is still increasing at the longest span leading-edge flap investigated ( $0.525b/2$ ).

Table I shows that for the rotated split, step split, and triangular flaps the largest values of  $C_{L_{max}}$  are obtained with the leading-edge flaps extending from the wing tip inboard to at least the wing midsemispan.

As shown in figure 8, the values of  $C_{L_{max}}$  for comparable leading- and trailing-edge flap configurations are approximately equal, fuselage on or off. The tabulated values of  $C_{L_{max}}$  (table I) indicate that the variation of  $C_{L_{max}}$  with flap deflection, leading-edge flap span, and flap type is essentially the same with fuselage on or off.

Lift increment in linear lift range.- The lift increments (at  $\alpha = 8^\circ$ ) due to flap deflection are presented in figure 17 for the split and extended split flaps in combination with  $0.425b/2$  leading-edge flaps. For the  $0.45b/2$  split flap  $\Delta C_L$  increases at a decreasing rate with flap deflection up to the greatest deflection tested ( $60^\circ$ ). An increase of the split flap span to  $0.60b/2$  results in somewhat higher values of  $\Delta C_L$ , roughly 40 percent larger at  $15^\circ$  deflection and 25 percent larger at  $60^\circ$  deflection. The variation of  $\Delta C_L$  with deflection of the  $0.60b/2$  flaps is similar to that for the shorter-span flaps. The addition of the leading-edge flaps, varying in span from  $0.375b/2$  to  $0.525b/2$ , results in an average increase of  $\Delta C_L$  of about 0.01, as shown in table I.



It is of interest to note that  $\Delta C_L$ , reduced by the  $\cos^2 \Lambda$ , produced by  $0.60b/2$  split flaps deflected  $60^\circ$  on the unswept-wing - fuselage combination of reference 3 is identical with that obtained with a similar flap configuration in the present tests.

The increment of lift coefficient resulting from deflection of the  $0.45b/2$  extended split flaps reaches a maximum at a deflection of about  $45^\circ$  and decreases from this maximum at higher deflections (fig. 17). Below  $30^\circ$ ,  $\Delta C_L$  for the extended split flaps is about twice that obtained with the split flaps.  $\Delta C_L$  is about the same for either the  $0.45b/2$  extended split flaps deflected  $30^\circ$  or the  $0.60b/2$  split flaps deflected  $60^\circ$ .

The lift characteristics of the wing-fuselage combination with the triangular, rotated split, and step split flaps are shown in figures 8 and 9. The value of  $\Delta C_L$  produced by the triangular flaps deflected  $30^\circ$  is about equal to that obtained with  $0.45b/2$  extended split flaps deflected  $30^\circ$  (table I). The effectiveness of the rotated split and step split flaps deflected  $45^\circ$  in producing an increase in lift at a constant angle of attack is generally between that of the split and extended split flaps. For example, the increment produced by the rotated split flaps is about 0.31 as compared with 0.37 for the extended split flaps and 0.22 for the split flaps. The step-type flaps in the forward position, however, produce the smallest increment (0.19) of all the flaps investigated. The addition of the separator plate between the two portions of the step flaps increases the value of  $\Delta C_L$  by 0.03 to about the same as the split flaps. The effectiveness of the step-type flap located in the rearward position is considerably increased and is about the same as that of the  $0.60b/2$  split flaps.

Of the split-type flaps investigated, then, the largest values of  $C_{L_{max}}$  and  $\Delta C_L$  are obtained with the flaps at moderate deflection angles and with those flaps having the hinge lines located on or near the wing trailing edge.

#### Pitching-Moment Characteristics

The pitching-moment characteristics of the model for representative flap configurations are shown in figures 9 to 14. A summary of the pitching-moment characteristics of the configurations investigated is presented in table II. Reference 4 has shown that extended leading-edge flaps of suitable span effectively delay the inherent stalling of the outer portions of the subject wing to high angles of attack so that a stable break of the pitching-moment curve results. Just prior to

maximum lift, however, various degrees of instability are encountered. The following discussion is primarily concerned with the effects of trailing-edge flaps on the direction of the moment break at maximum lift and on the degree of instability just prior to maximum lift.

As shown in figures 10 and 11, the direction of the break in the pitching-moment curve near maximum lift is practically unaffected by the degree of deflection of the trailing-edge flaps. The addition of the trailing-edge flaps to the model equipped with certain spans of leading-edge flap is, in many cases, effective in reducing the initial unstable variation of pitching-moment coefficient with lift coefficient which is present in the high-lift range below maximum lift. In particular, those flaps which tend to increase the wing area are most effective in reducing this unstable variation. For example, the wing-fuselage combination with  $0.375b/2$  leading-edge flaps exhibits an initial unstable change in the longitudinal stability parameter,  $dC_m/dC_L$ , of approximately 0.18. The addition of the  $0.45b/2$  extended split flaps and split flaps deflected  $30^\circ$  reduces this change to about 0.02 and 0.10, respectively. With the flap spans increased to  $0.60b/2$ , however, the unstable change is only reduced to 0.15 and 0.17 for extended split flaps and split flaps, respectively.

The degree of deflection of the trailing-edge flaps also affects the magnitude of this initial instability. For each flap type there is usually one flap deflection angle for which the contribution of the flap to stability in the range under consideration is the largest. The optimum flap deflection usually is about  $30^\circ$  to  $45^\circ$  for the flaps investigated (figs. 10 and 11). Deflection angles less than or greater than the aforementioned deflection range generally are not as effective and for some configurations actually increase the original flap-off instability.

Examples of the effectiveness of the leading-edge flaps in controlling the pitching moment at or near maximum lift are shown in figures 12 and 13. Without the leading-edge flaps, the moment curve breaks sharply unstable. The addition of either the  $0.375b/2$  or  $0.425b/2$  leading-edge flaps results in a stable break of the moment curve in this high-lift range near  $C_{L_{max}}$ . Progressively increasing the leading-edge flap span beyond  $0.425b/2$  results in the model again becoming unstable. In general, table II shows that the maximum span of leading-edge flap, for which stable moment characteristics in the high-lift range near  $C_{L_{max}}$  are obtained, is limited for the wing-fuselage combination to about  $0.475b/2$ . As shown in reference 4, the maximum leading-edge flap span, which provides stability of the wing alone in the high-lift range near  $C_{L_{max}}$ , is dependent to a slight degree upon the



trailing-edge flap type. For the wing-fuselage combination tested herein the maximum leading-edge flap span from stability considerations is also affected slightly by the type of trailing-edge flap. As illustrated in table II, a stable break in the pitching-moment curve at  $C_{L_{max}}$  is obtained for the wing-fuselage combination equipped with the rotated split flaps with a leading-edge flap  $0.050b/2$  longer than that used with the other trailing-edge flap configurations.

As one indication of the comparative usefulness of the various types of flaps investigated, the highest lift coefficients obtained before the onset of destabilizing moment changes are presented in table II. It can be seen that with the  $0.45b/2$  extended split flaps in combination with the  $0.375b/2$  leading-edge flaps, stable variations of pitching moment were obtained up to a lift coefficient of 1.38 at  $30^\circ$  deflections. The corresponding value of lift coefficient obtained with the  $0.60b/2$  extended split flaps is approximately 0.10 less and with the remaining types of flap nearly 0.40 less. The comparatively high value obtained with the  $0.45b/2$  extended split flaps is a result of the virtual elimination of the unstable moment characteristics prior to the final stable break of the pitching-moment curve. For several of the  $0.45b/2$  extended split flap configurations having stable characteristics at  $C_{L_{max}}$ , values of  $C_{L_{max}}$  of up to 1.50 are obtained with a destabilizing change in  $dC_m/dC_L$  of less than 0.05. With the  $0.60b/2$  extended split flaps, values of  $C_{L_{max}}$  up to 1.65 are obtained with changes of less than 0.15 (fig. 13).

The increments of pitching-moment coefficient resulting from flap deflection were measured at  $C_L = 0.8$  for the various flaps deflected  $45^\circ$ . Because short flap spans are involved and the inboard location on the sweptback wing places them longitudinally near to the assumed center of gravity, the trim changes obtained are small. The greatest trim change occurring with the  $0.45b/2$  flaps amounts to an increment of pitching-moment coefficient of about -0.07 for the extended split flap. With the  $0.60b/2$  extended split flaps the increment increases to only -0.11.

A change in stability in the low-lift range corresponding to a 3 or 4 percent forward shift of the aerodynamic center is the primary result of the addition of the fuselage to the wing (fig. 14).

### Drag Characteristics

Representative drag data are presented in figures 15 and 16 for a few configurations. In order to illustrate more clearly the effects of flap deflection, span, and type on the drag characteristics, the lift-drag ratios and the gliding characteristics are presented in figures 19 to 21.

The effects of the degree of deflection of the split flaps are shown in figure 19. In the low and moderate lift range the lift-drag ratios are largest for the wing-fuselage combination without trailing-edge flaps or with the trailing-edge flaps at low deflections. At a lift coefficient of about 1.05 the L/D values are approximately equal except for the flaps-off condition for which the values are somewhat lower. It can be seen from the chart of gliding speed against sinking speed that at gliding speeds of 125 to 130 miles per hour, which correspond to about 120 percent of the minimum speed of the wing-fuselage combination at sea level with an assumed wing loading of 40 pounds per square foot, minimum values of sinking speed are obtained with flap deflections of  $15^\circ$  and  $30^\circ$ .

The effects of increasing the flap span from  $0.45b/2$  to  $0.60b/2$  are also shown in figure 19. At gliding speeds of 125 to 130 miles per hour, increasing the flap span reduces the sinking speed slightly for the  $15^\circ$  flap deflection and increases it slightly for the  $60^\circ$  deflection. The difference in glide angles for the speed range under consideration does not exceed  $2^\circ$  or  $3^\circ$  regardless of the flap deflection or span.

The effects of the degree of deflection of the extended split flaps are shown in figure 20. In the gliding range of 120 to 125 miles per hour, which corresponds to 120 percent of the minimum speed, the minimum values of sinking speed occur also at deflections of  $15^\circ$  and  $30^\circ$ . For equal deflections the sinking speeds are approximately equal for either the  $0.45b/2$  or the  $0.60b/2$  flap configurations, although the gliding speeds at 120 percent of the minimum speed are slightly different. In this speed range the maximum difference in the sinking speed for flap deflections of  $15^\circ$  to  $60^\circ$  and spans of  $0.45b/2$  to  $0.60b/2$  is 4 feet per second.

The relative drag characteristics of the various flaps are shown in figure 21. Above a lift coefficient of about 1.05 the values of L/D are lowest for the split flaps, highest for the extended split flaps, and intermediate for the rotated split flaps and the optimum configuration of the step split flaps (rearward position with separator plate). Throughout the lift range the values of L/D of the triangular flaps are slightly lower than those of the extended split flaps.



The chart of gliding characteristics in figure 21 indicates that at the landing-approach speed, for the case under consideration, the sinking speeds are only slightly affected by the flap type.

#### Comparison with Flaps of the Slotted Type

The results of tests of single and double slotted flaps on the subject wing, obtained from unpublished data, are compared in figures 22 and 23 with the results of tests of the extended split flaps. The configuration used for the comparison consists of the wing-fuselage combination equipped with  $0.475b/2$  leading-edge flaps and the  $0.45b/2$  trailing-edge flaps deflected  $30^\circ$ .

The maximum lift coefficient produced by the double slotted flap configuration is slightly higher than that produced by either the extended split flaps or the single slotted flaps, about 1.57 compared to 1.52 and 1.49, respectively. For a given angle of attack the lift increment produced by the double slotted flaps is slightly larger than that of the other flaps. The changes in longitudinal trim due to flap deflection are about the same for the double slotted and extended split flaps and slightly less for the single slotted flaps. The moment characteristics at maximum lift are similar. The glide characteristics, as illustrated in figure 23, are nearly identical in the high-lift, low-speed range.

The preceding comparison is based on equal spans ( $0.45b/2$ ) of the extended split, single slotted, and double slotted flaps and, on this basis, the effectiveness of the extended split flaps is nearly the same as that of the double slotted flaps. Reference 4 has indicated that for this wing without a fuselage, longer spans of split flap than of double slotted flap may be employed when the criterion for allowable flap span is stable pitching-moment characteristics at  $C_{L_{max}}$ . As it has been shown herein that the addition of the fuselage has little effect at  $C_{L_{max}}$  on the stability of the wing equipped with either the split or the extended split flaps, it is likely that on this same stability basis longer spans of extended split flap than of double slotted flap may be used. With an increased span of extended split flap, it is probable that the resulting lift effectiveness would be greater than that of the double-slotted-flap configuration.

## CONCLUDING REMARKS

From the results of an investigation in the Langley 19-foot pressure tunnel to determine the effects of split-type flaps on a  $47.7^\circ$  sweptback-wing - fuselage combination, the following remarks can be made:

1. Of the split-type flaps investigated the largest values of maximum lift coefficient  $C_{L_{\max}}$  and increment in lift coefficient due to flap deflection  $\Delta C_L$  are obtained at deflection angles of the order of  $40^\circ$  with those flaps having hinge lines located on or near the wing trailing edge.

2. When the wing is equipped with leading-edge flaps, the longitudinal stability in the high-lift range below  $C_{L_{\max}}$  is dependent upon the trailing-edge flap type and the degree of flap deflection.

3. A value of  $C_{L_{\max}}$  of 1.50 is obtained on a wing configuration with 0.45-semispan extended split flaps in combination with 0.425-semispan extended leading-edge flaps. This configuration has stable pitching-moment characteristics at  $C_{L_{\max}}$  and destabilizing changes in the slope of the pitching-moment curve  $dC_m/dC_L$  of less than 0.05 below  $C_{L_{\max}}$ . With the span of the extended split flaps increased to 0.60 semispan, a value of  $C_{L_{\max}}$  of 1.65 is obtained with a change in  $dC_m/dC_L$  of less than 0.15.

4. From considerations of  $C_{L_{\max}}$ , lift-drag ratio, and longitudinal stability, the effectiveness of the extended split flaps is about equal to that of double slotted flaps of the same span.

Langley Aeronautical Laboratory  
National Advisory Committee for Aeronautics  
Langley Field, Va.



## REFERENCES

1. Spooner, Stanley H., and Mollenberg, Ernst F.: Positioning Investigation of Single Slotted Flaps on a  $47.7^\circ$  Sweptback Wing at Reynolds Numbers of  $4.0 \times 10^6$  and  $6.0 \times 10^6$ . NACA RM L50H29, 1950.
2. Eisenstadt, Bertram J.: Boundary-Induced Upwash for Yawed and Swept-Back Wings in Closed Circular Wind Tunnels. NACA TN 1265, 1947.
3. Sivells, James C., and Spooner, Stanley H.: Investigation in the Langley 19-Foot Pressure Tunnel of Two Wings of NACA 65-210 and 64-210 Airfoil Sections with Various Type Flaps. NACA Rep. 942, 1949. (Formerly NACA TN 1579.)
4. Salmi, Reino J.: Effects of Leading-Edge Devices and Trailing-Edge Flaps on Longitudinal Characteristics of Two  $47.7^\circ$  Sweptback Wings of Aspect Ratios 5.1 and 6.0 at a Reynolds Number of  $6.0 \times 10^6$ . NACA RM L50F20, 1950.

TABLE I.- SUMMARY OF THE LIFT CHARACTERISTICS OF THE WING AND WING-FUSELAGE  
COMBINATION WITH VARIOUS FLAP CONFIGURATIONS.

Trailing-edge flap			Fuse- lage	$C_{Lmax}$					$\Delta C_L (\alpha = 8^\circ)$					
Type	Span (b/2)	$\delta_f$ (deg)		Leading-edge flap span										
				0	0.375	0.425	0.475	0.525	0	0.375	0.425	0.475	0.525	
Flaps off	—	—	On	1.16	<sup>a</sup> 1.36	<sup>a</sup> 1.41	1.44	1.45	—	0.01	0.01	0.01	0.01	
Split	0.45	30	off	1.27	—	1.43	1.50	—	0.22	—	.24	.24	—	
				1.30	—	1.39	1.44	—	.29	—	.31	.29	—	
		On	15	1.20	1.39	1.43	1.47	1.46	.10	.10	.11	.10	.10	
			30	1.19	1.40	1.45	1.50	1.47	.16	.17	.17	.16	.18	
			45	1.16	1.34	1.37	1.45	1.46	.21	.21	.22	.22	.22	
			60	1.17	1.32	1.34	1.39	1.43	.24	.24	.25	.25	.26	
	0.60	15	1.21	<sup>a</sup> 1.40	<sup>a</sup> 1.46	<sup>a</sup> 1.50	1.51	.13	.14	.14	.14	.14		
		30	1.23	<sup>a</sup> 1.42	1.51	<sup>a</sup> 1.59	1.53	.21	.23	.22	.23	.22		
		45	1.19	<sup>a</sup> 1.38	1.45	1.49	1.49	.27	.28	.28	.27	.28		
		60	1.19	<sup>a</sup> 1.34	1.38	1.44	1.48	.30	.32	.31	.32	.31		
	Extended split	0.45	30	off	—	1.43	1.50	1.57	1.58	—	.41	.43	.41	.42
					15	1.31	1.43	1.45	1.50	1.51	.18	.18	.18	.19
On			30	1.34	<sup>a</sup> 1.46	<sup>a</sup> 1.49	1.52	1.55	.30	.31	.32	.32	.32	
			45	1.35	1.46	1.50	1.54	1.57	.33	.36	.37	.37	.37	
0.60		30	On	1.34	1.45	1.49	1.51	1.55	.32	.33	.33	.33	.34	
				1.38	1.55	1.65	1.65	1.68	.39	.40	.41	.41	.41	
		45	1.39	1.59	1.70	1.70	1.67	.46	.46	.46	.45	.47		
			1.39	1.59	1.70	1.70	1.67	.46	.46	.46	.45	.47		
Rotated split	0.45	45	off	1.25	1.37	<sup>a</sup> 1.45	1.46	1.46	.40	.41	.41	.41	.42	
			on	—	1.41	1.44	1.45	1.49	—	.31	.31	.32	.32	
Triangular	—	15	off	1.25	1.41	1.44	1.46	1.46	.25	.25	.25	.25	.25	
				30	1.30	1.41	1.44	1.46	1.46	.43	.44	.43	.45	.43
		On	45	1.28	1.42	1.42	1.44	1.55	.38	.38	.38	.39	.39	
			30	—	1.46	1.47	1.50	1.55	—	.30	.30	.30	.30	
Step split (forward position)	0.45	45	On	—	<sup>a</sup> 1.27	1.31	1.33	1.35	—	.19	.19	.20	.20	
Step split with separator plate (forward position)				—	<sup>a</sup> 1.28	1.30	1.35	1.33	—	.22	.23	.23	.24	
Step split (rearward position)				—	1.38	1.43	1.49	1.49	—	.28	.29	.28	.28	
Step split with separator plate (rearward position)				—	1.41	1.45	1.45	1.50	—	.30	.30	.31	.31	

<sup>a</sup>  $C_L$  still increasing at highest  $\alpha$  tested.

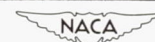
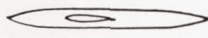
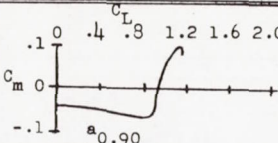
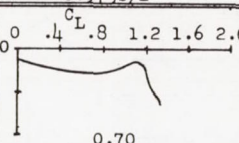
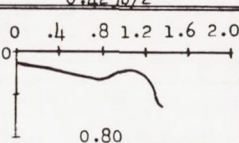
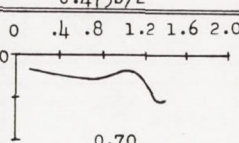
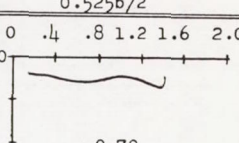

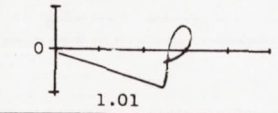
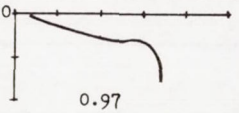
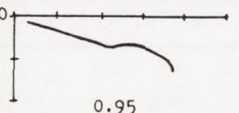

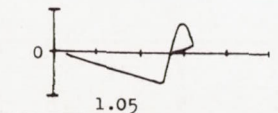
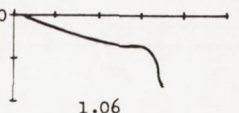
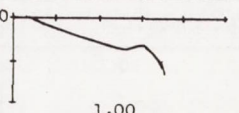
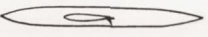
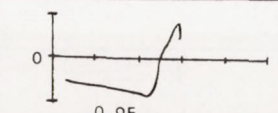
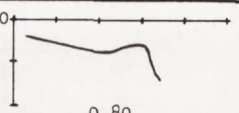
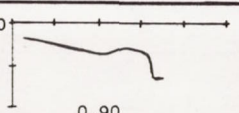
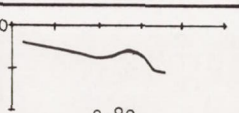
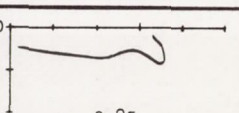
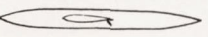
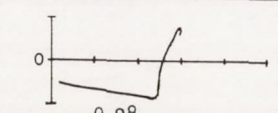
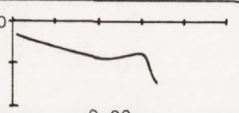
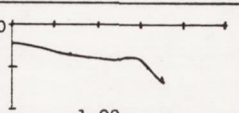
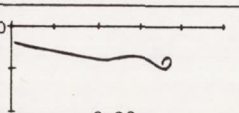
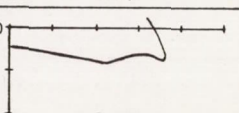
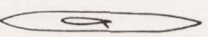
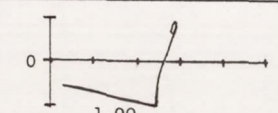
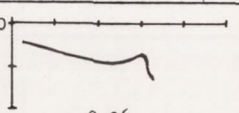
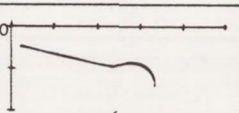
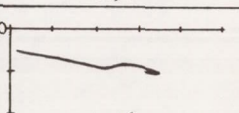
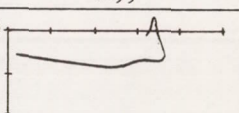
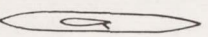
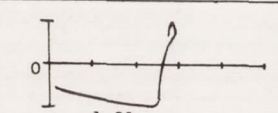
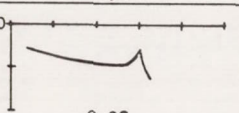
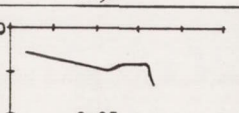
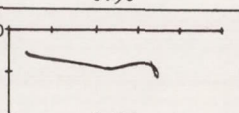
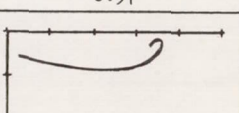




TABLE II.- SUMMARY OF THE PITCHING-MOMENT CHARACTERISTICS OF THE WING AND WING-FUSELAGE COMBINATION WITH VARIOUS FLAP CONFIGURATIONS

Configuration	$\delta_f$	Leading-Edge Flap Span				
		0	$0.375b/2$	$0.425b/2$	$0.475b/2$	$0.525b/2$
 Flaps off	off	 0.90 <sup>a</sup>	 0.70	 0.80	 0.70	 0.70
 0.45b/2 split	30°	 1.01		 0.97	 0.95	
 0.45b/2 split	45°	 1.05		 1.06	 1.00	
 0.45b/2 split	15°	 0.95	 0.80	 0.90	 0.80	 0.85
 0.45b/2 split	30°	 0.98	 0.90	 1.00	 0.90	 0.95
 0.45b/2 split	45°	 1.00	 0.96	 0.96	 0.96	 0.97
 0.45b/2 split	60°	 1.01	 0.92	 0.95	 0.97	 1.00

<sup>a</sup> Lift coefficient at initial break in moment curve.

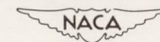


TABLE II.- (Continued)


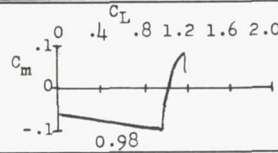
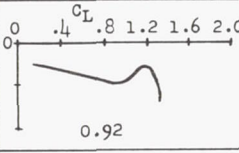
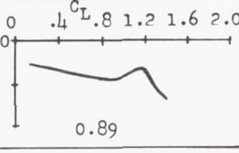
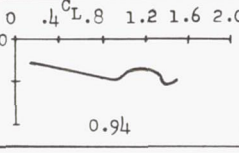
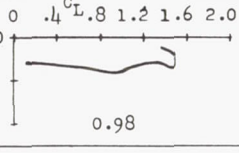
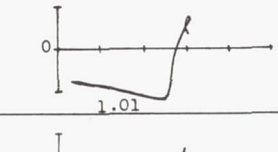
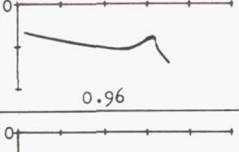
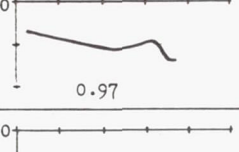
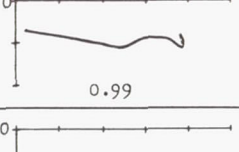
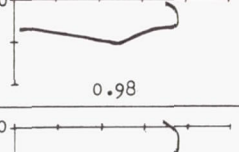
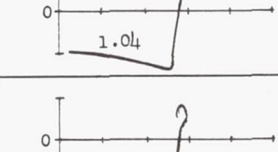
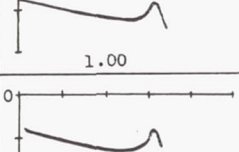
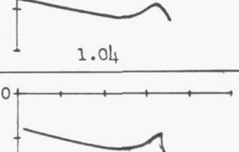
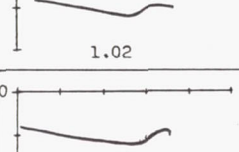
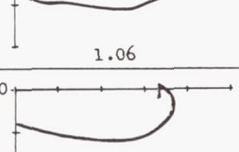
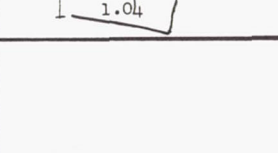
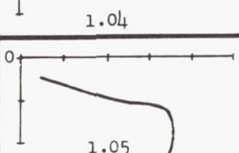
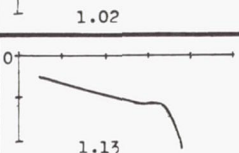
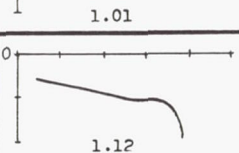
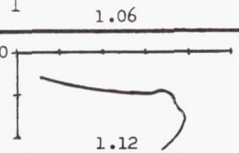

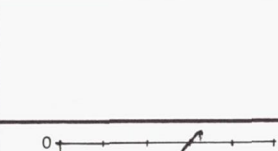
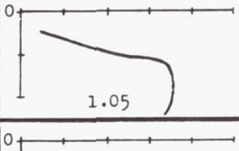
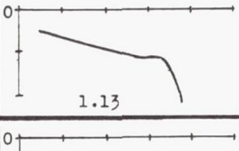
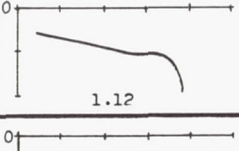

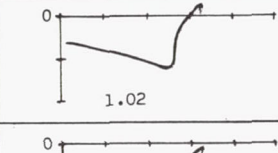
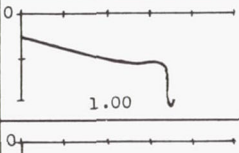
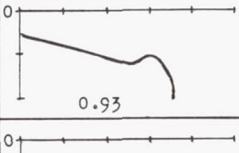
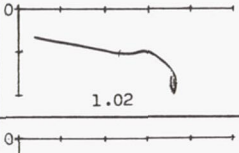
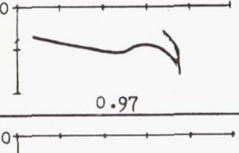
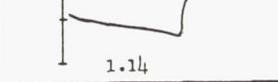
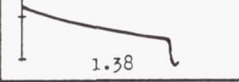
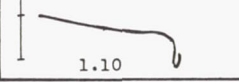

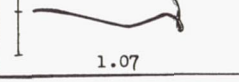
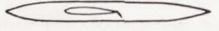
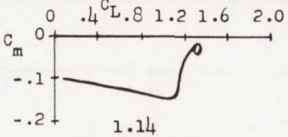
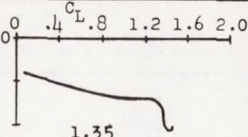
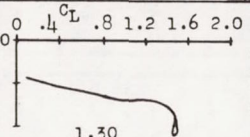
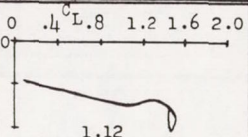
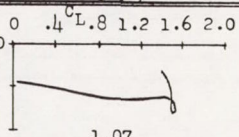
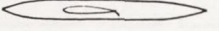
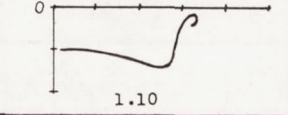
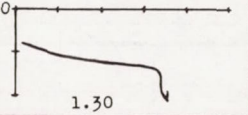
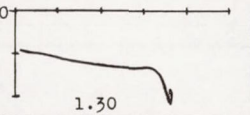
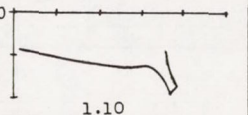
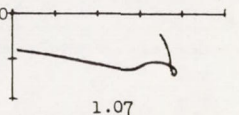
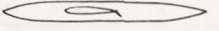
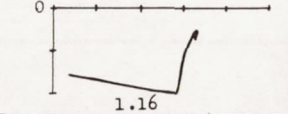
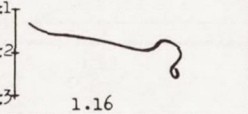
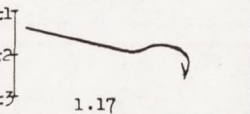
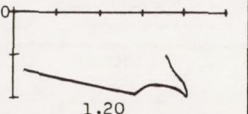
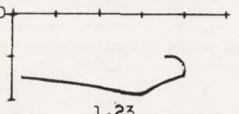
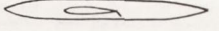
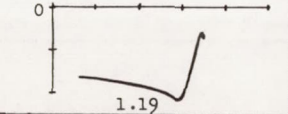
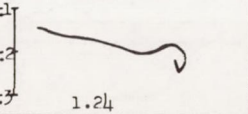
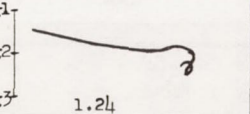
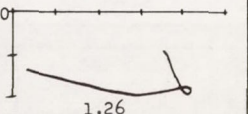
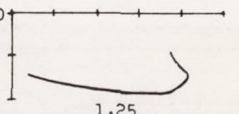
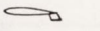
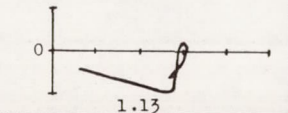
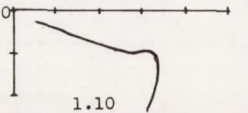
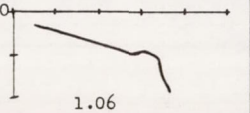
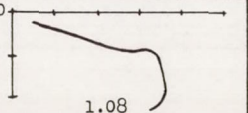
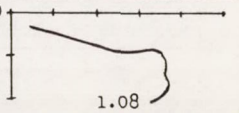
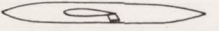
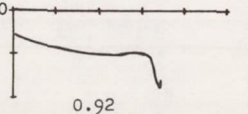
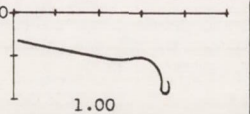
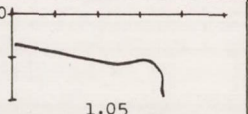
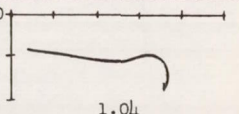
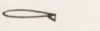
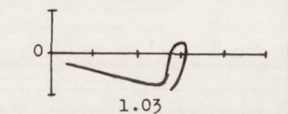
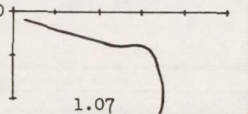
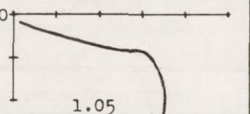
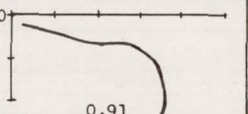
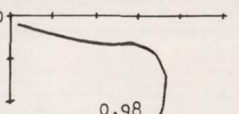
Configuration	$\delta_f$	Leading-Edge Flap Span				
		0	$0.375b/2$	$0.425b/2$	$0.475b/2$	$0.525b/2$
 .60b/2 split	15°	 0.98	 0.92	 0.89	 0.94	 0.98
	30°	 1.01	 0.96	 0.97	 0.99	 0.98
	45°	 1.04	 1.00	 1.04	 1.02	 1.06
	60°	 1.04	 1.04	 1.02	 1.01	 1.06
	30°	 .45b/2 extended split	 1.05	 1.13	 1.12	 1.12
 .45b/2 extended split	15°	 1.02	 1.00	 0.93	 1.02	 0.97
	30°	 1.14	 1.38	 1.10	 1.08	 1.07





TABLE II.- (Continued)

Configuration	$\delta_f$	Leading-Edge Flap Span				
		0	$0.375b/2$	$0.425b/2$	$0.475b/2$	$0.525b/2$
 0.45b/2 extended split	45°	 1.14	 1.35	 1.30	 1.12	 1.07
	60°	 1.10	 1.30	 1.30	 1.10	 1.07
 0.60b/2 extended split	30°	 1.16	 1.16	 1.17	 1.20	 1.23
	45°	 1.19	 1.24	 1.24	 1.26	 1.25
 0.45b/2 rotated split	45°	 1.13	 1.10	 1.06	 1.08	 1.08
 0.45b/2 rotated split	45°		 0.92	 1.00	 1.05	 1.04
 Triangular	15°	 1.03	 1.07	 1.05	 0.91	 0.98

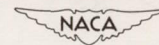

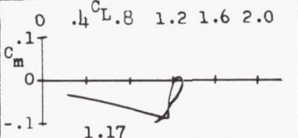
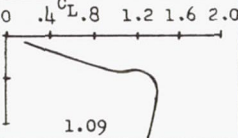
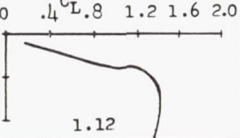
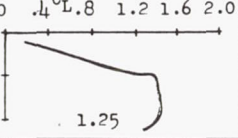
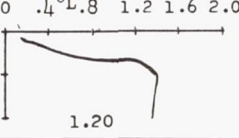
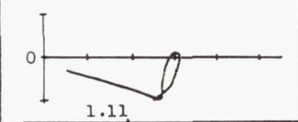
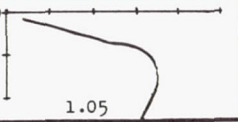
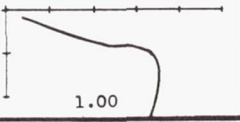
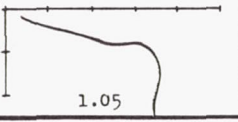
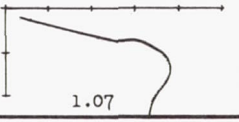

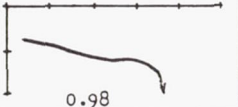
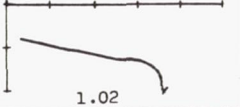
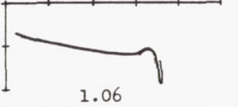
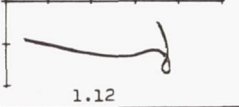
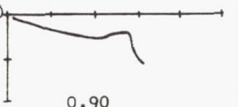
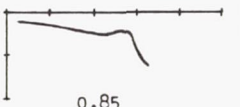
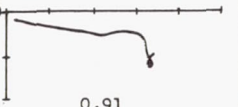
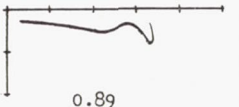

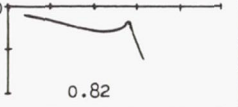
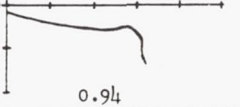
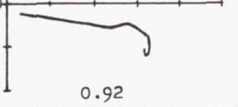
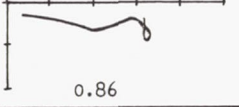
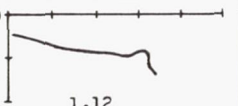

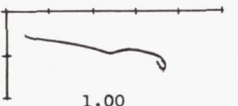
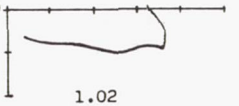
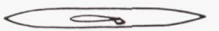
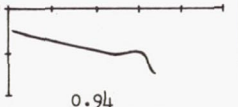
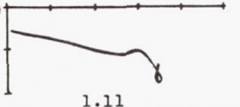
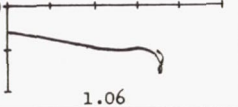
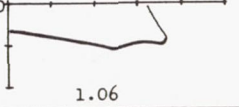


TABLE II.- (Concluded)

Configuration	$\delta_f$	Leading-Edge Flap Span				
		0	$0.375b/2$	$0.425b/2$	$0.475b/2$	$0.525b/2$
 Triangular	30°	 1.17	 1.09	 1.12	 1.25	 1.20
	45°	 1.11	 1.05	 1.00	 1.05	 1.07
 Triangular	30°		 0.98	 1.02	 1.06	 1.12
	45°		 0.90	 0.85	 0.91	 0.89
 .45b/2 step split with separator plate (forward position)	45°		 0.82	 0.94	 0.92	 0.86
	45°		 1.12	 0.93	 1.00	 1.02
 .45b/2 step split with separator plate (rearward position)	45°		 0.94	 1.11	 1.06	 1.06
	45°					





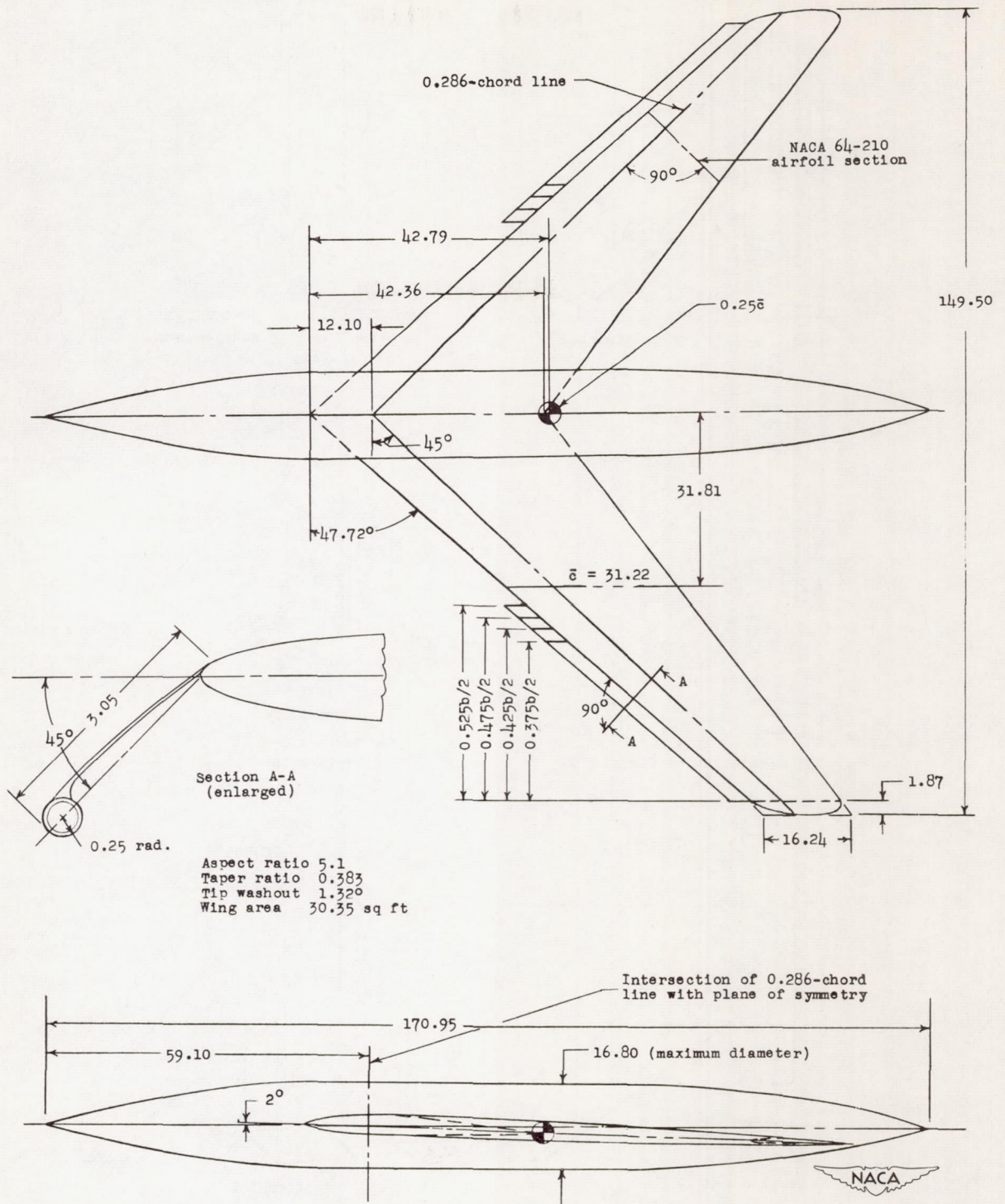


Figure 1.- Geometry of the 47.7° sweptback-wing - fuselage combination and details of the leading-edge flaps. All dimensions are in inches.

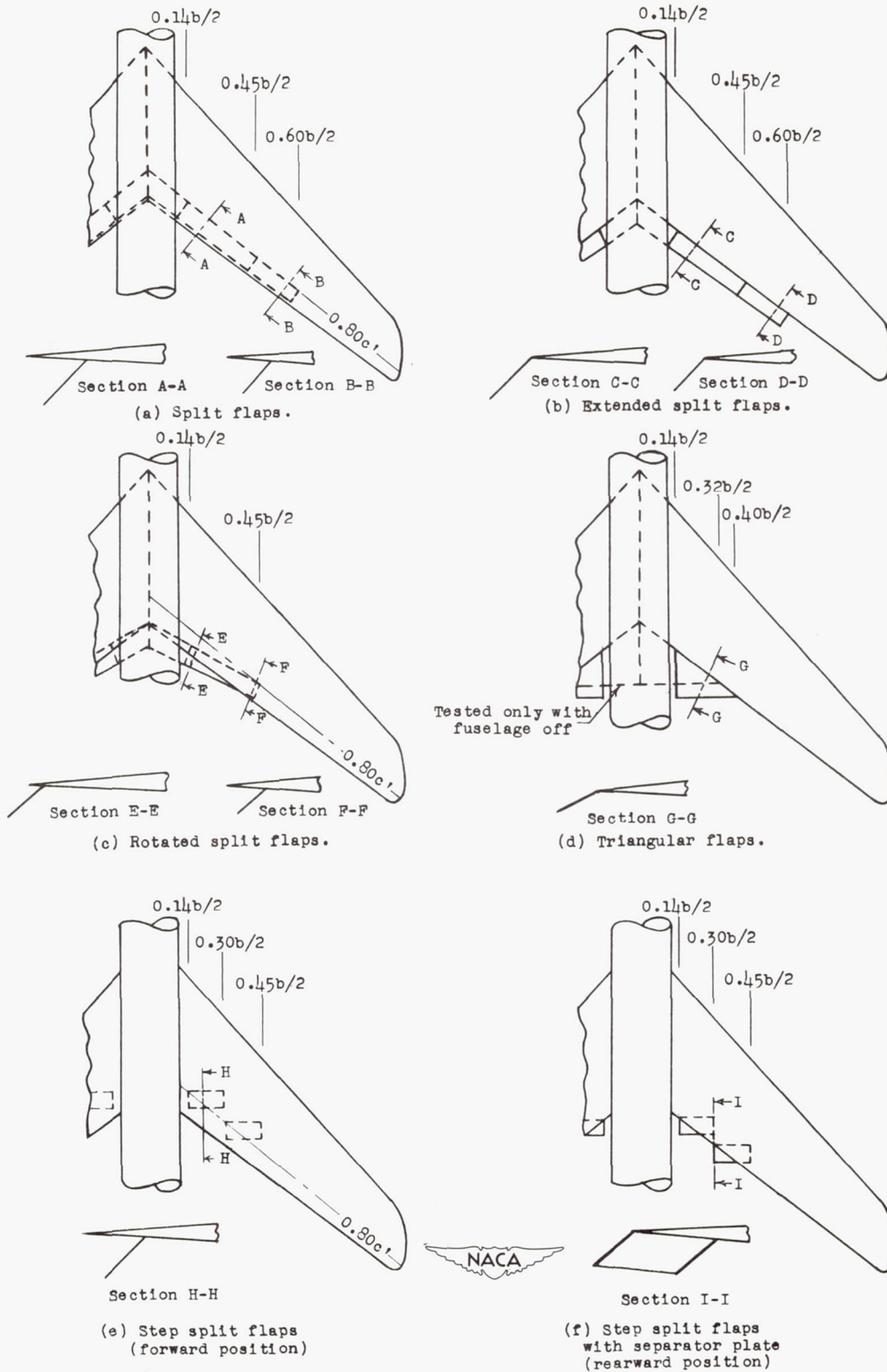


Figure 2.- Locations of the flaps on the wing and the wing-fuselage combination.



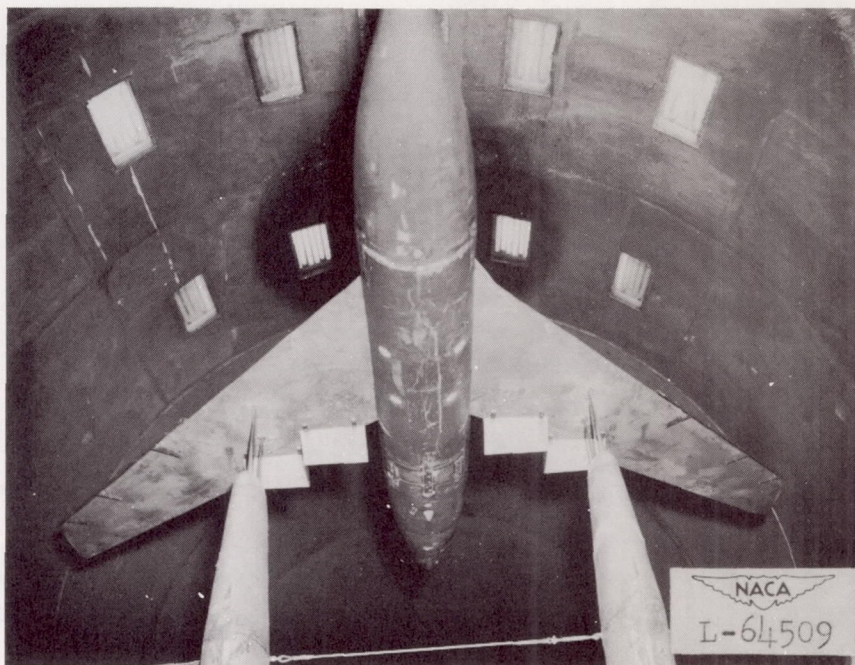


Figure 3.- The  $47.7^\circ$  sweptback-wing - fuselage combination mounted in the Langley 19-foot pressure tunnel.

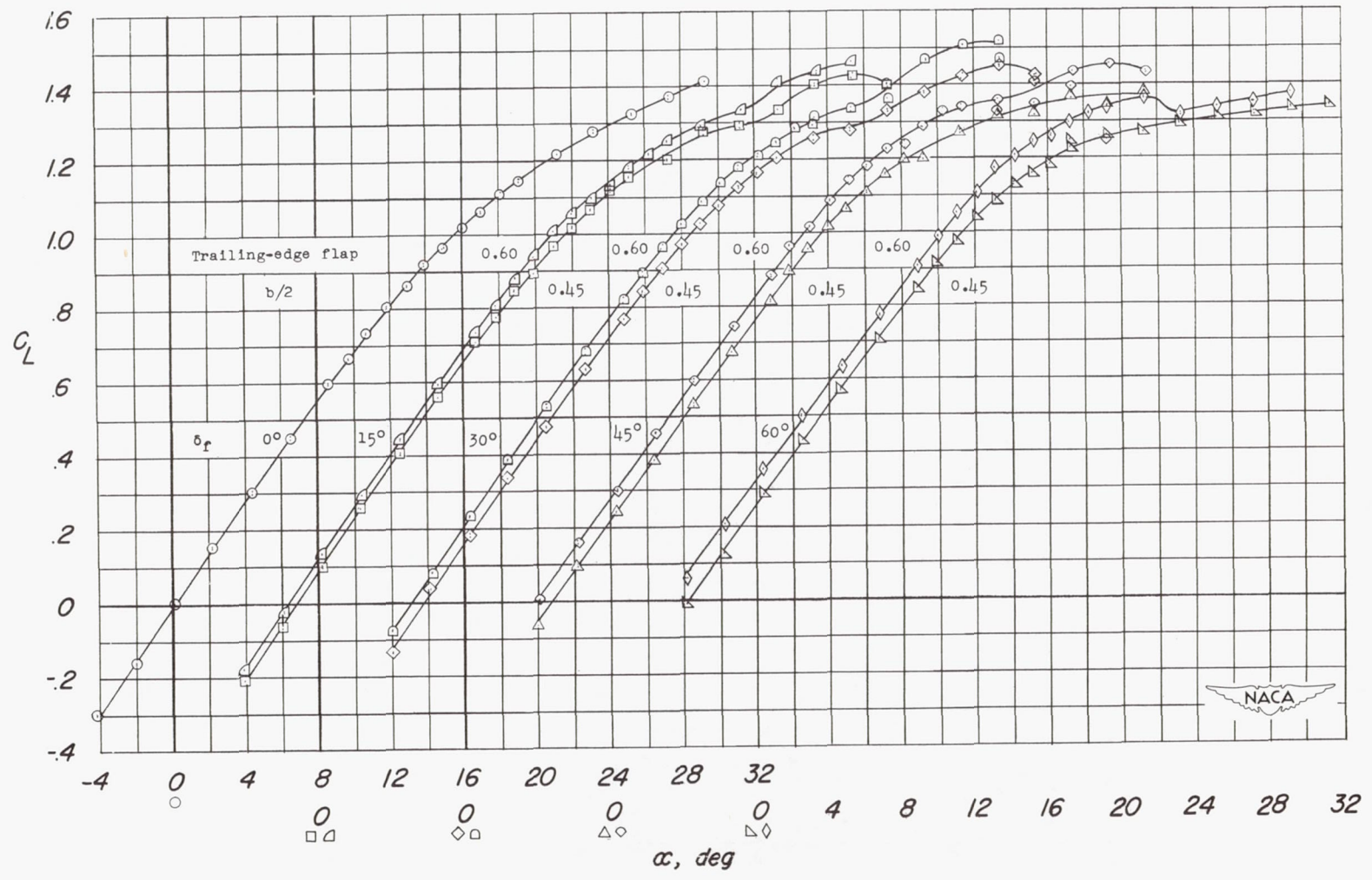


Figure 4.- Effects of deflection and span of the split flaps on the aerodynamic characteristics of the wing-fuselage combination equipped with 0.425b/2 leading-edge flaps.



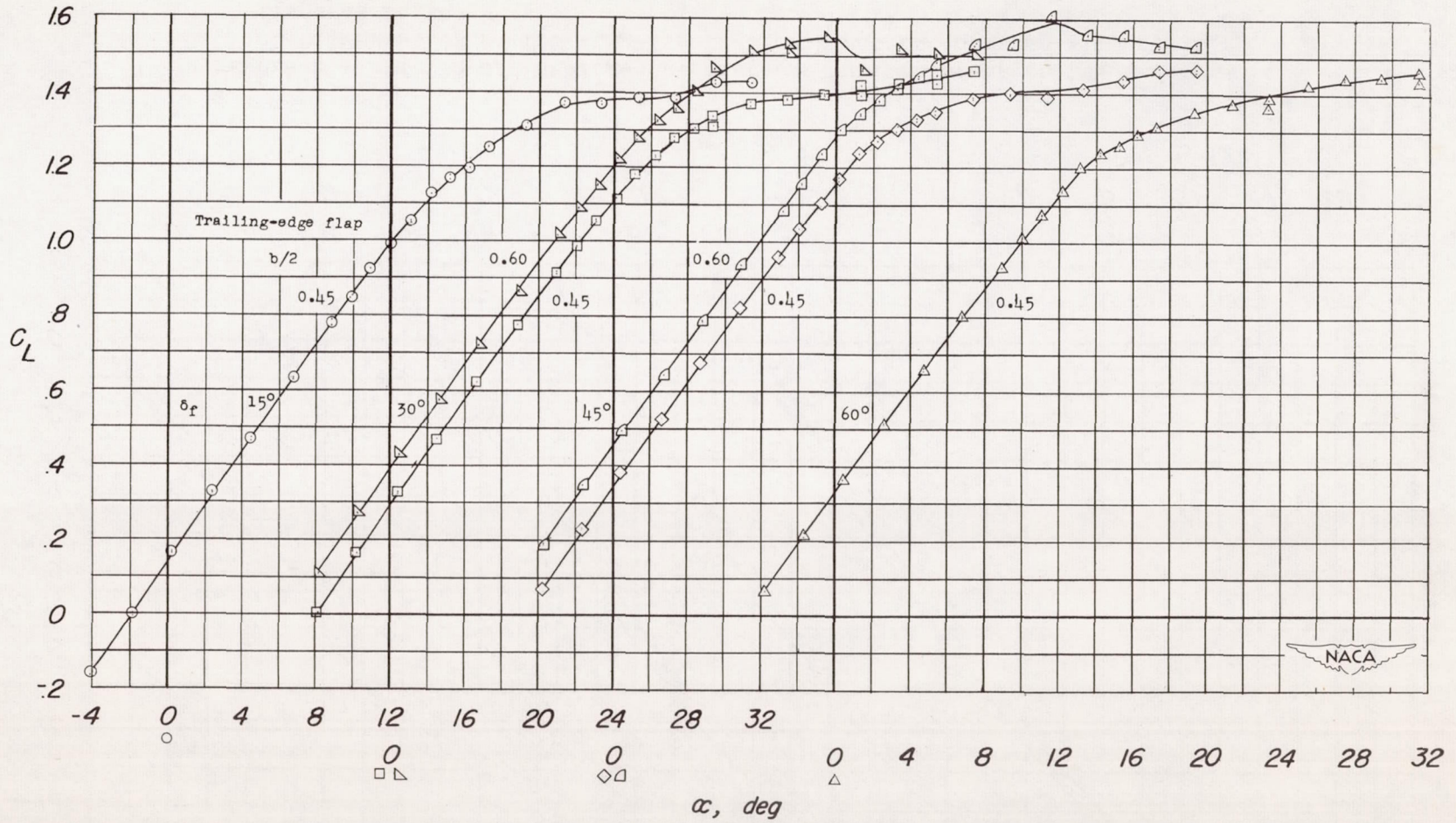


Figure 5.- Effects of deflection and span of the extended split flaps on the aerodynamic characteristics of the wing-fuselage combination equipped with  $0.375b/2$  leading-edge flaps.

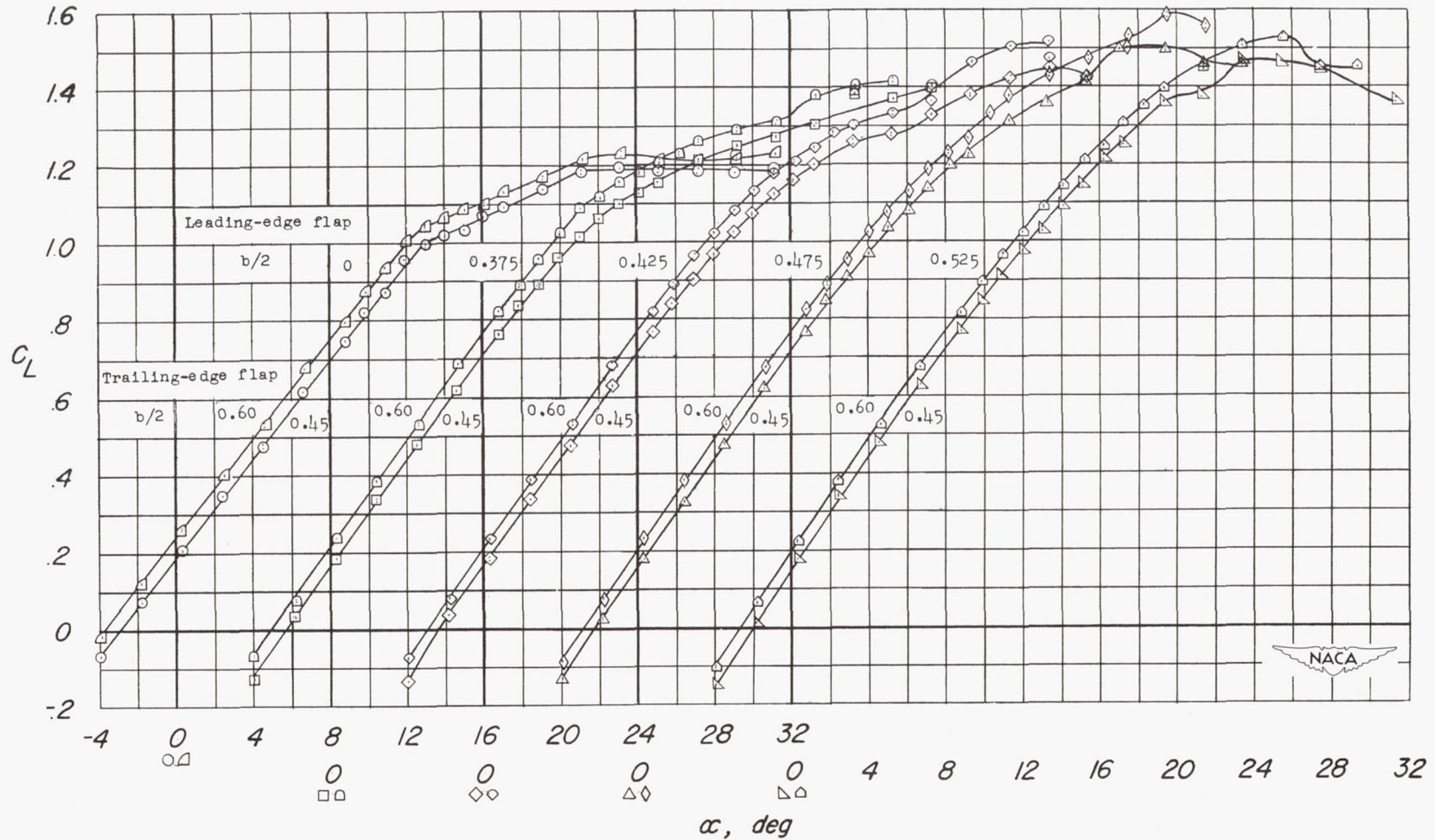


Figure 6.- Effects of leading-edge flaps of various spans on the aerodynamic characteristics of the wing-fuselage combination equipped with split flaps deflected  $30^\circ$ .



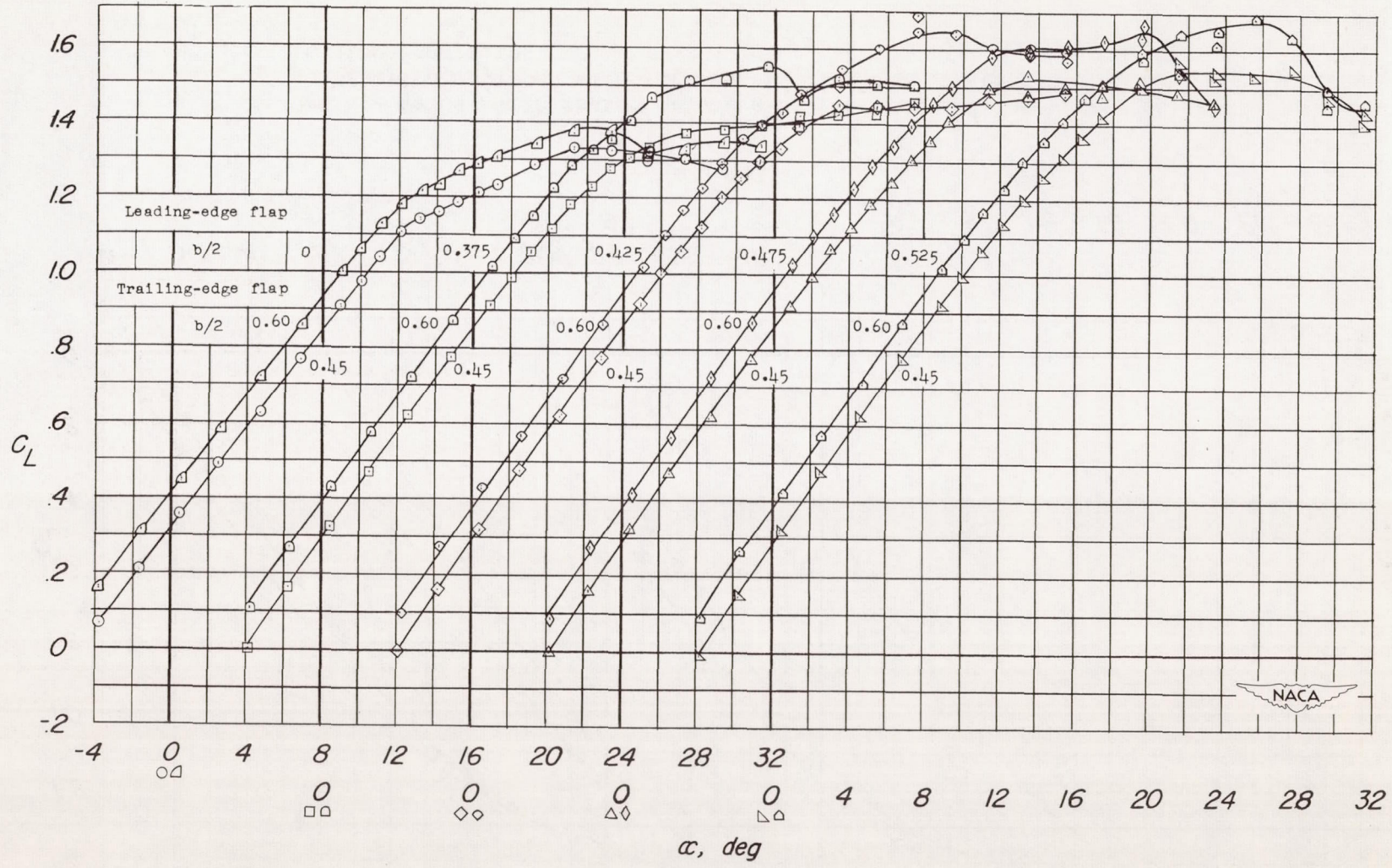


Figure 7.- Effects of leading-edge flaps of various spans on the aerodynamic characteristics of the wing-fuselage combination equipped with extended split flaps deflected  $30^\circ$ .

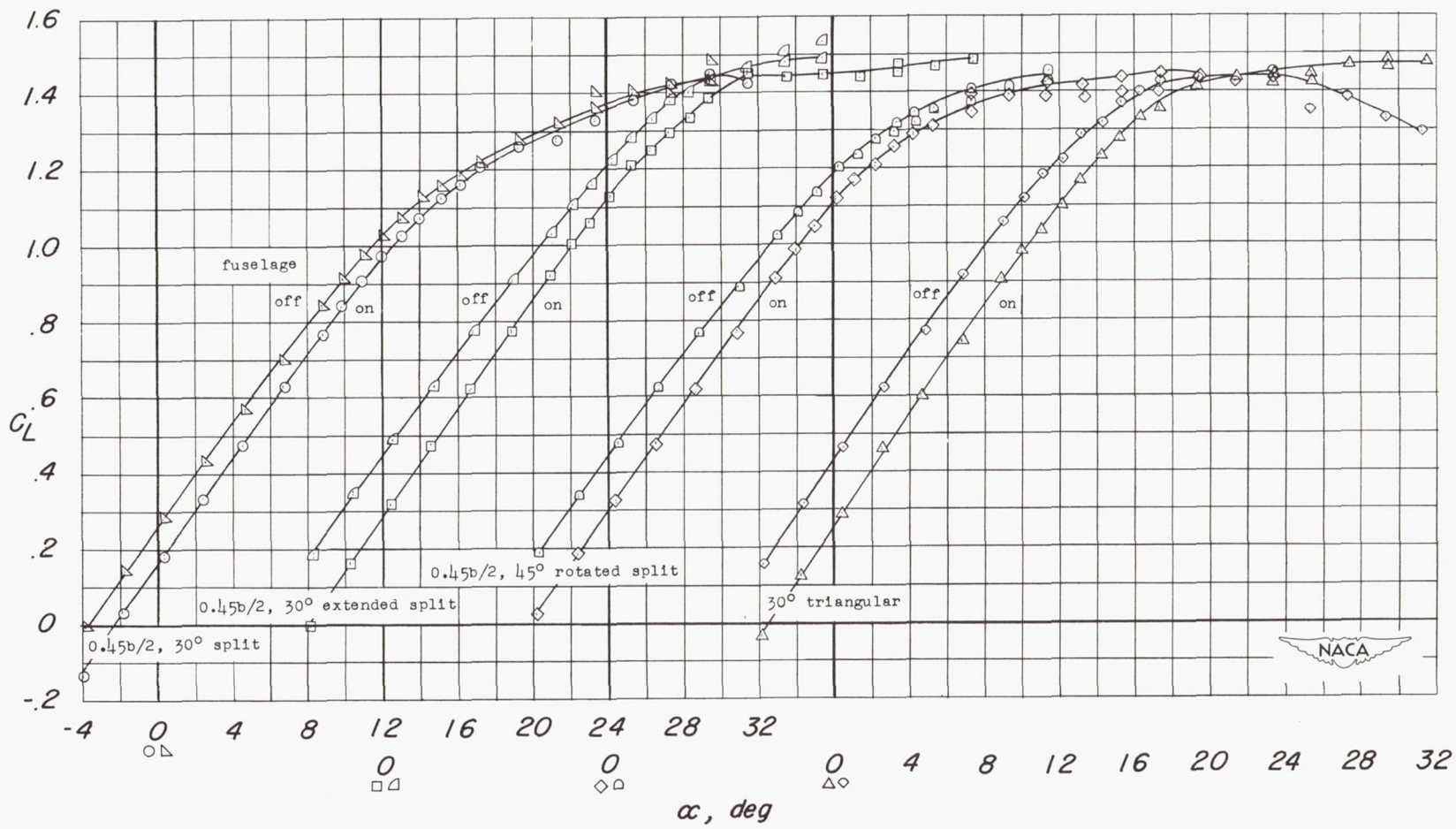


Figure 8.- Aerodynamic characteristics of the wing and the wing-fuselage combination equipped with various trailing-edge flaps and 0.425b/2 leading-edge flaps.



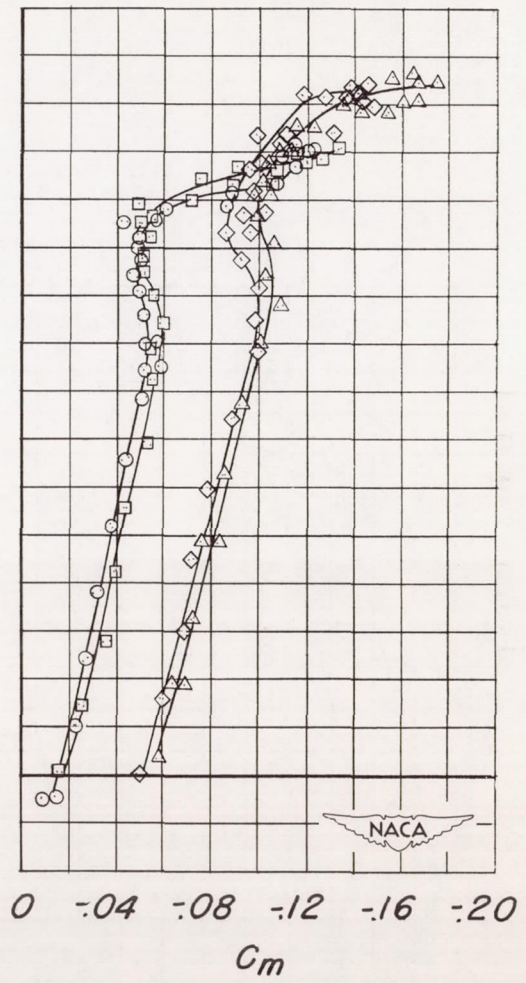
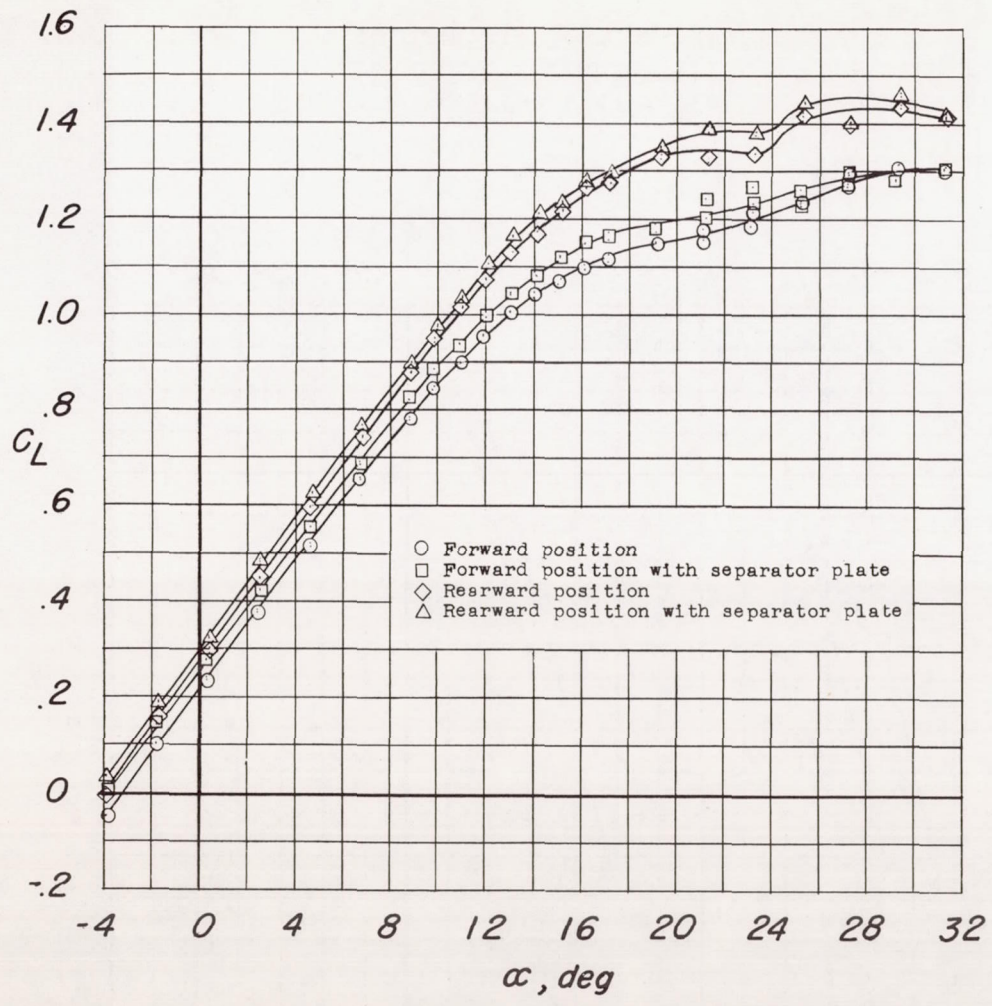


Figure 9.- Aerodynamic characteristics of the wing-fuselage combination equipped with the  $0.45b/2$  step split flaps deflected  $45^\circ$ .  $0.425b/2$  leading-edge flaps.

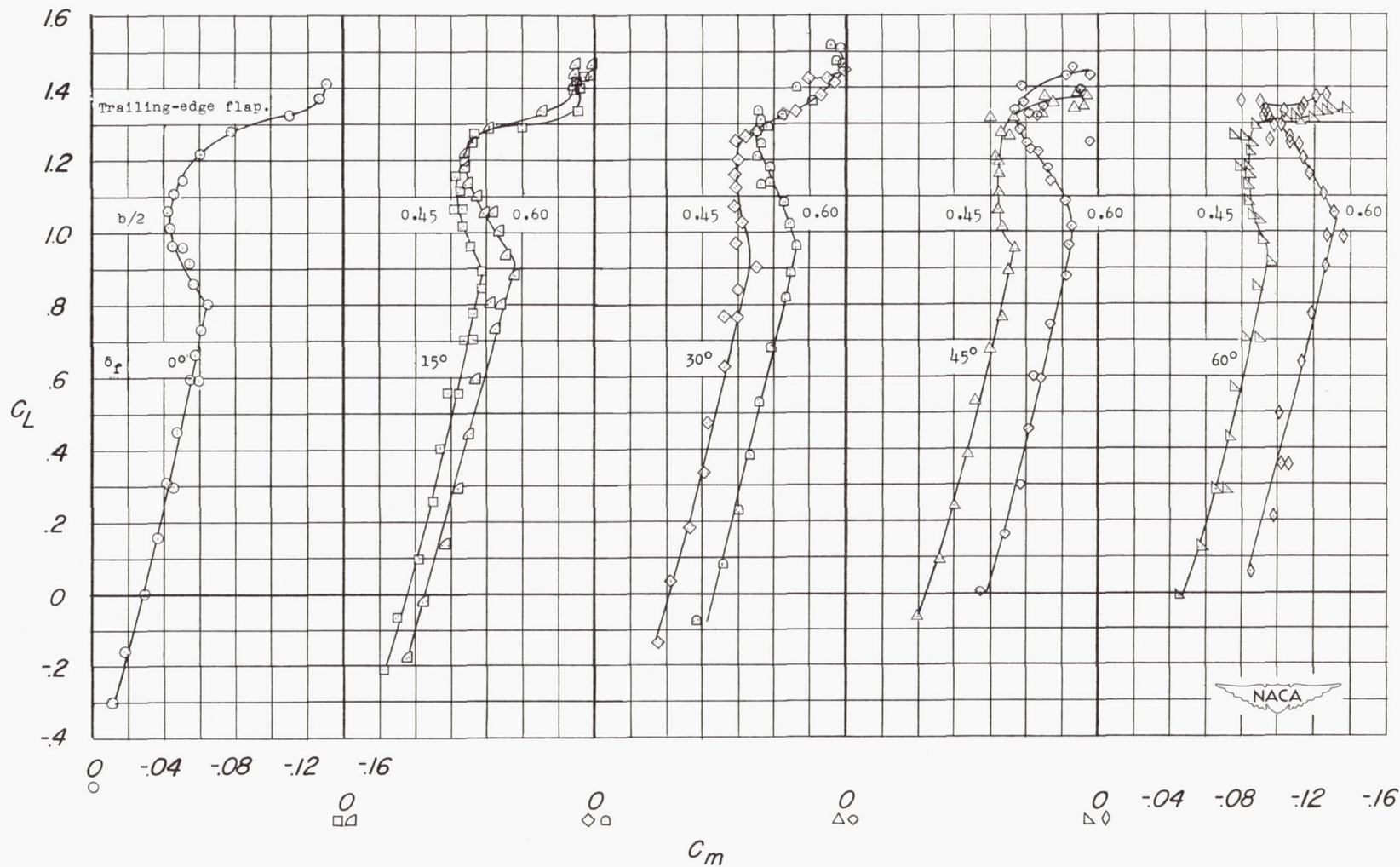


Figure 10.- Effects of deflection and span of the split flaps on the aerodynamic characteristics of the wing-fuselage combination equipped with  $0.425b/2$  leading-edge flaps.



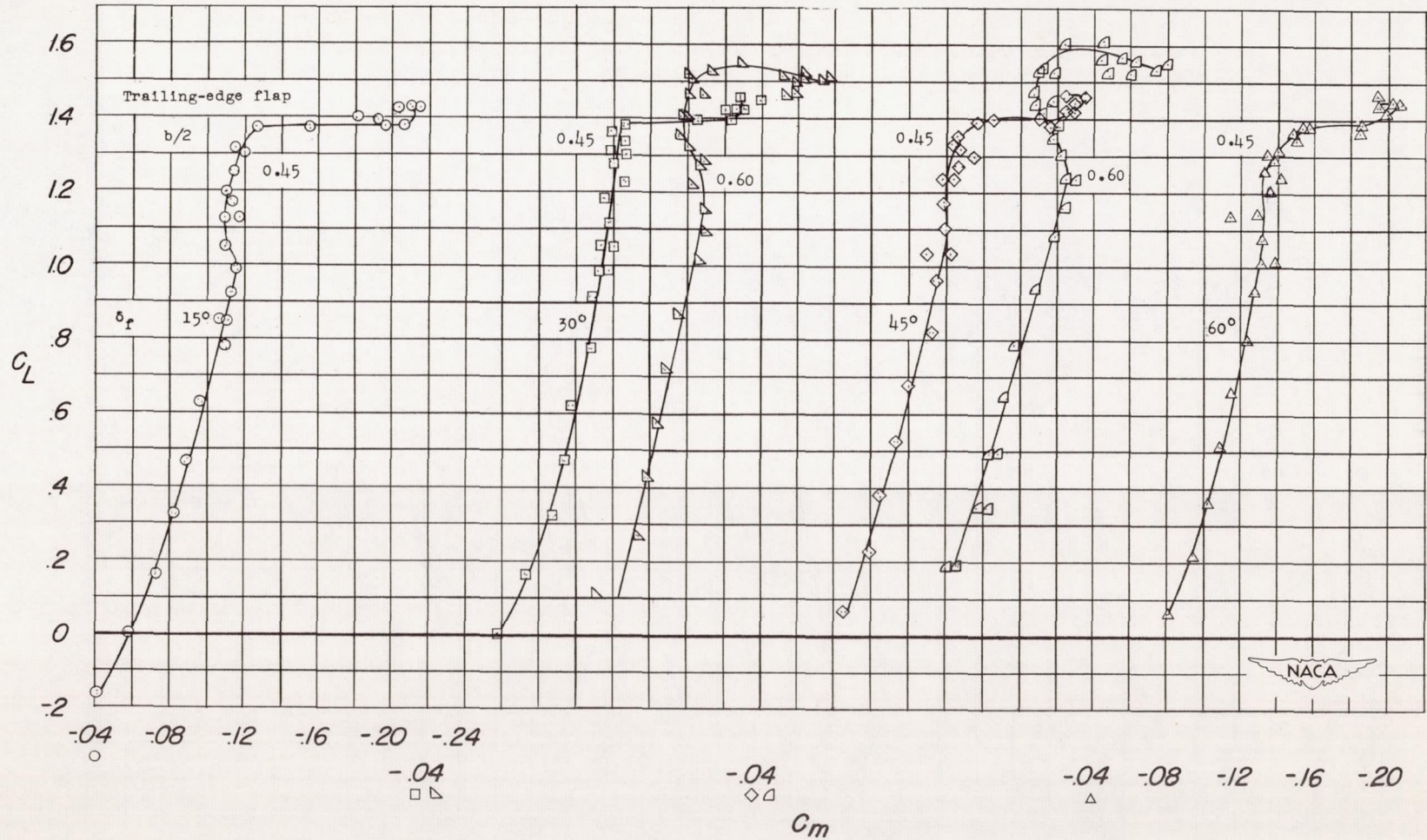


Figure 11.- Effects of deflection and span of the extended split flaps on the aerodynamic characteristics of the wing-fuselage combination equipped with  $0.375b/2$  leading-edge flaps.

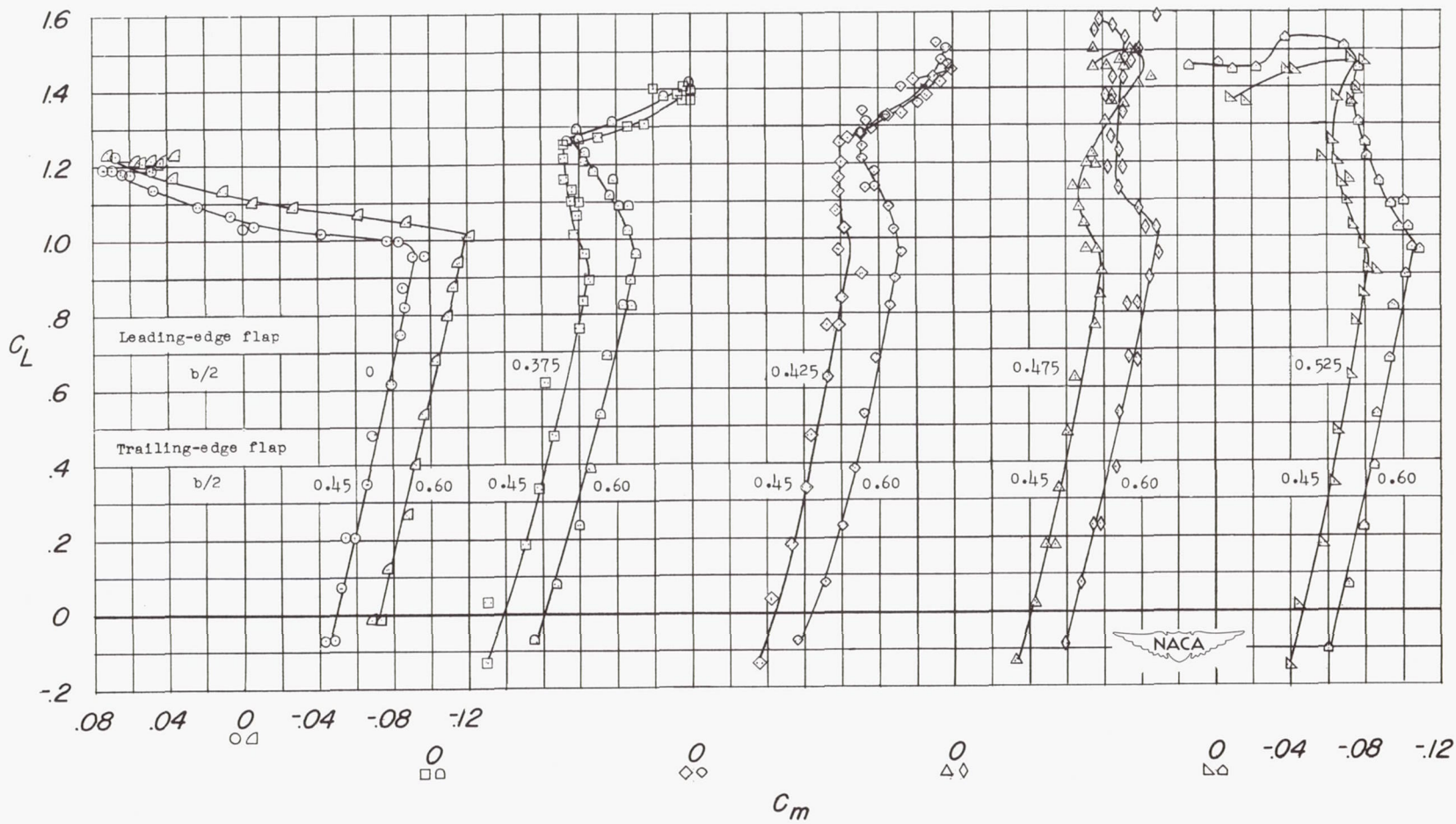


Figure 12.- Effects of leading-edge flaps of various spans on the aerodynamic characteristics of the wing-fuselage combination equipped with split flaps deflected  $30^\circ$ .



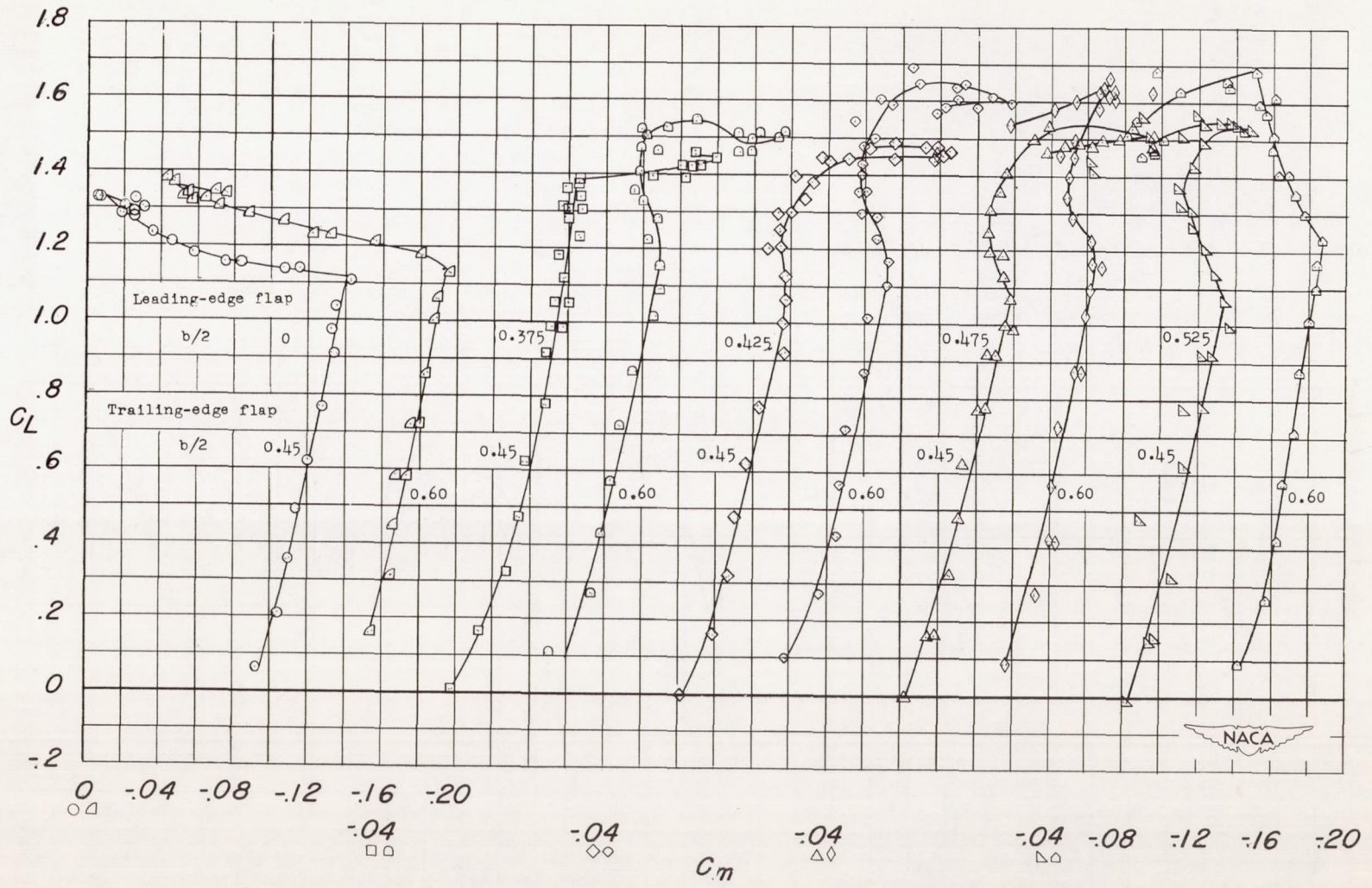


Figure 13.- Effects of leading-edge flaps of various spans on the aerodynamic characteristics of the wing-fuselage combination equipped with extended split flaps deflected  $30^\circ$ .

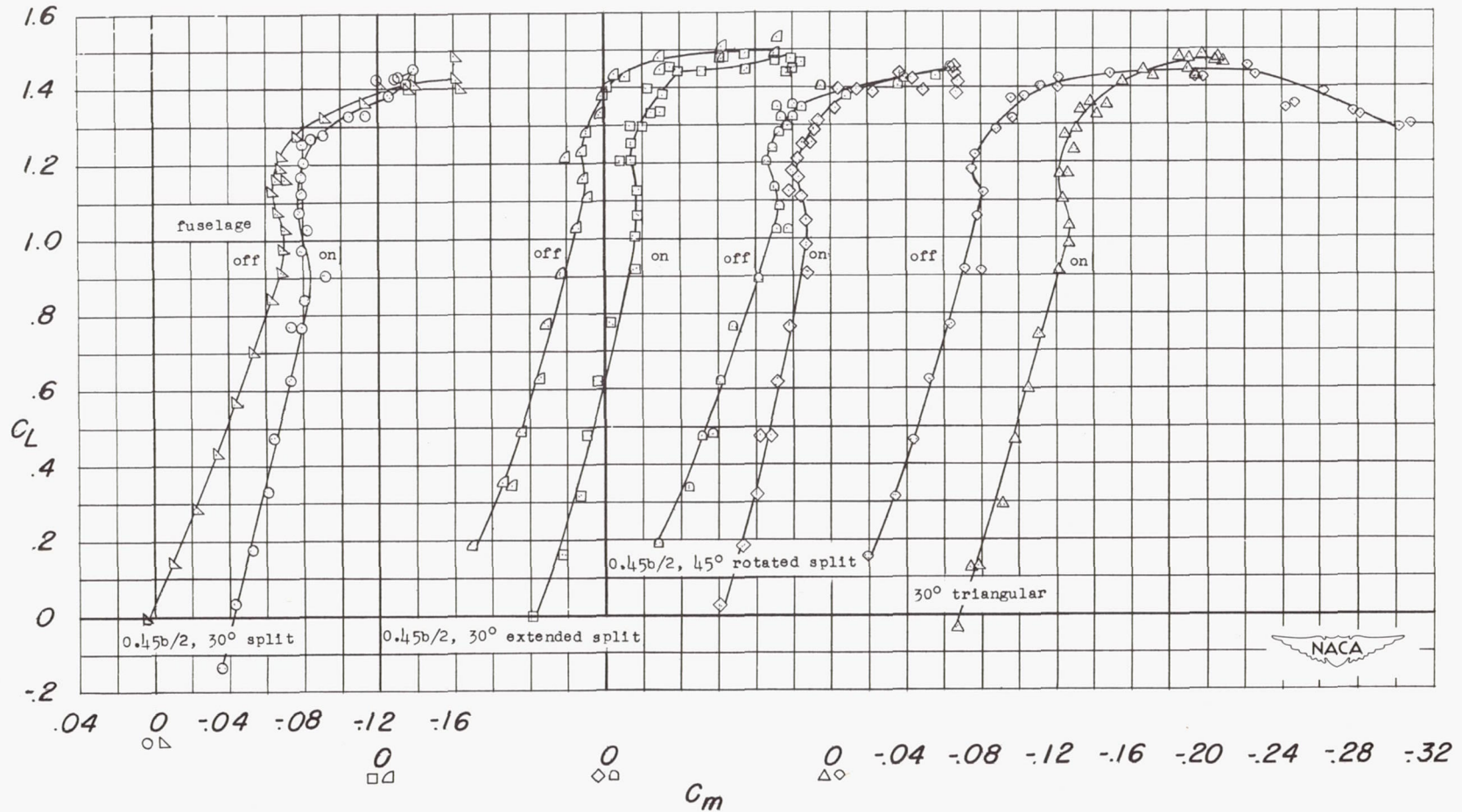


Figure 14.- Aerodynamic characteristics of the wing and the wing-fuselage combination equipped with various trailing-edge flaps and  $0.425b/2$  leading-edge flaps.



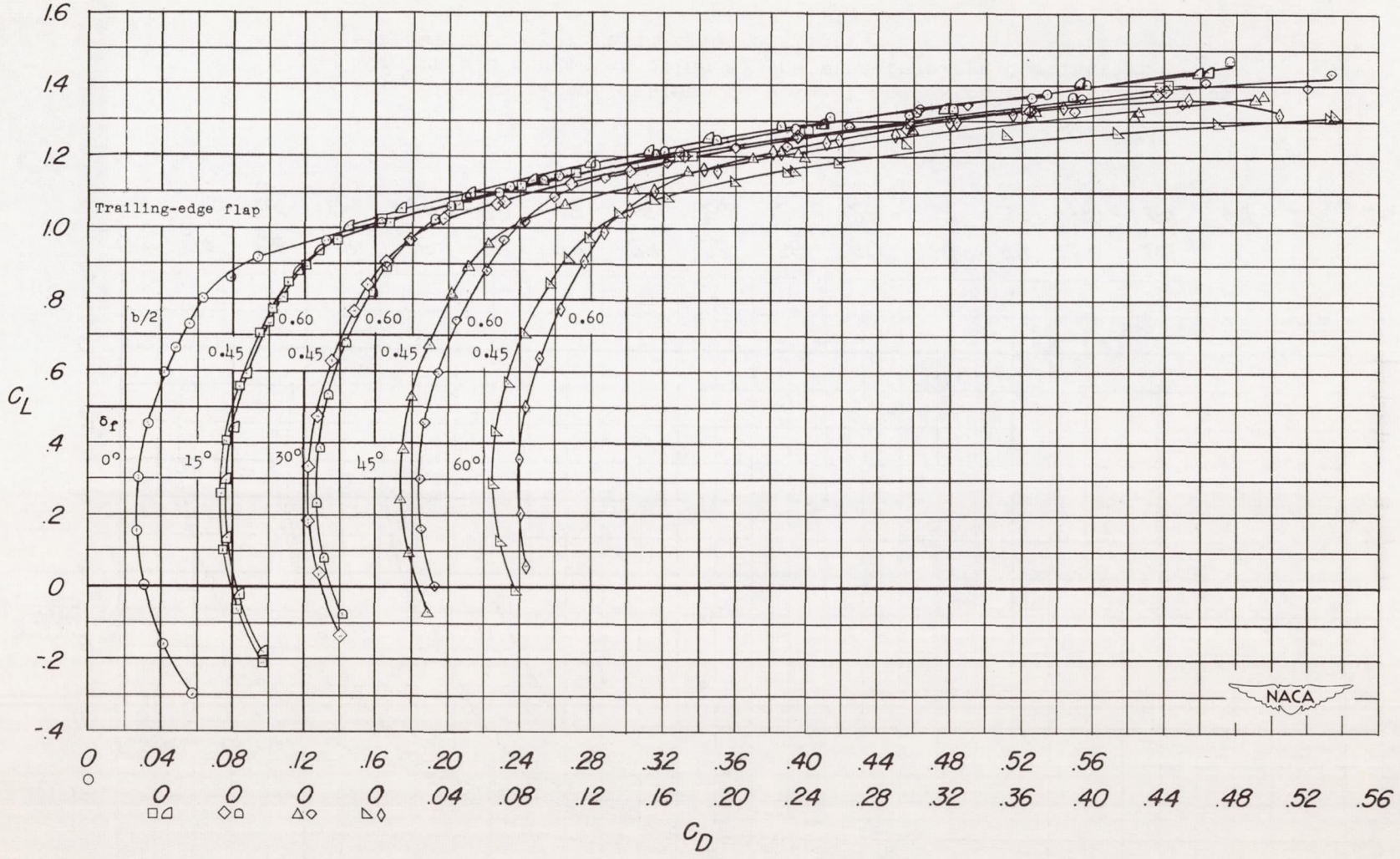


Figure 15.- Effects of deflection and span of the split flaps on the aerodynamic characteristics of the wing-fuselage combination equipped with 0.425b/2 leading-edge flaps.

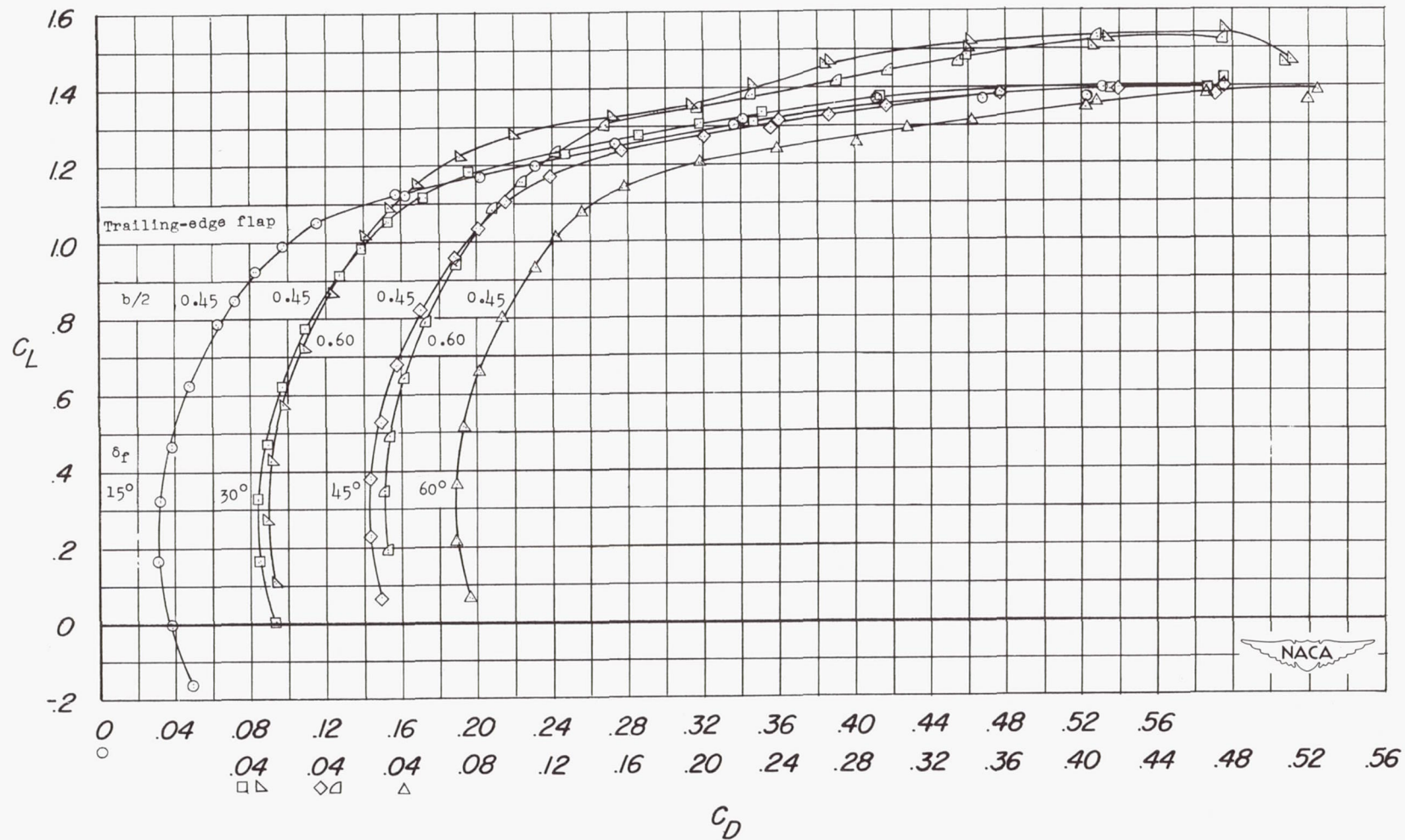
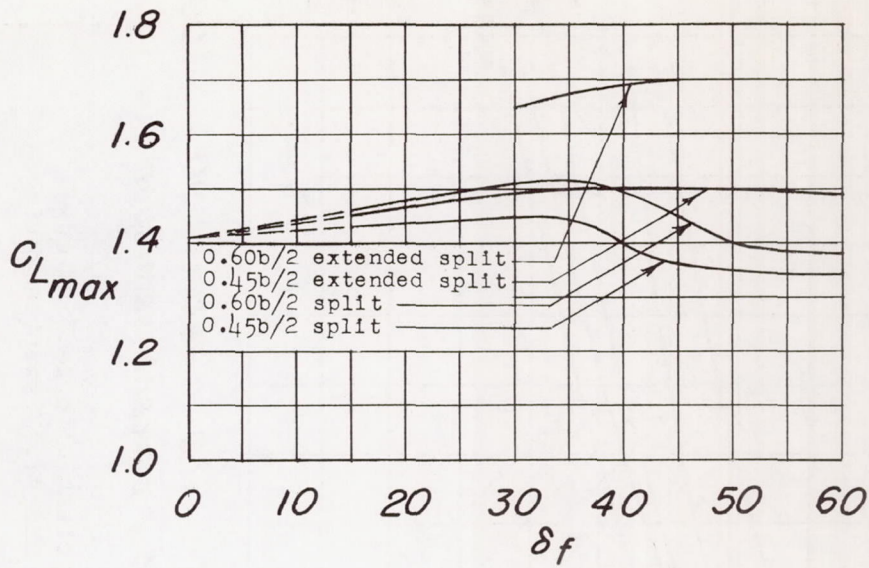
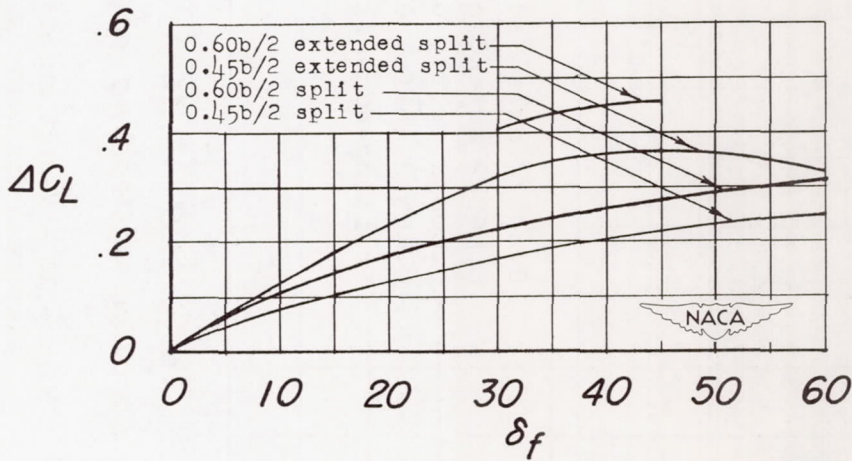


Figure 16.- Effects of deflection and span of the extended split flaps on the aerodynamic characteristics of the wing-fuselage combination equipped with 0.375b/2 leading-edge flaps.





(a)  $C_{L_{max}}$  against  $\delta_f$ .



(b)  $\Delta C_L$  against  $\delta_f$ .

Figure 17.- Variation of  $C_{L_{max}}$  and  $\Delta C_L$  with flap deflection on the  $47.7^\circ$  sweptback-wing - fuselage combination; 0.425b/2 leading-edge flaps.

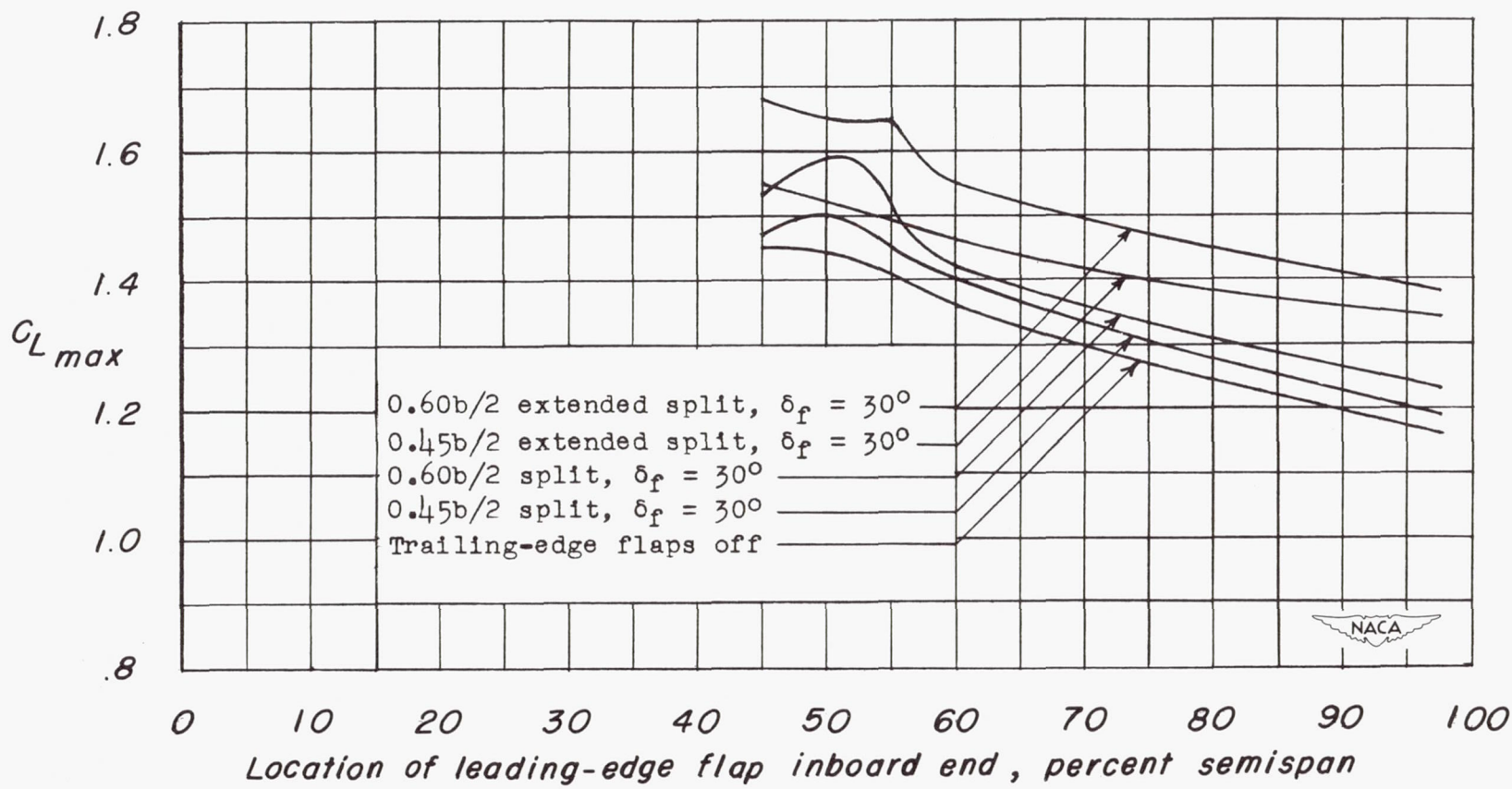
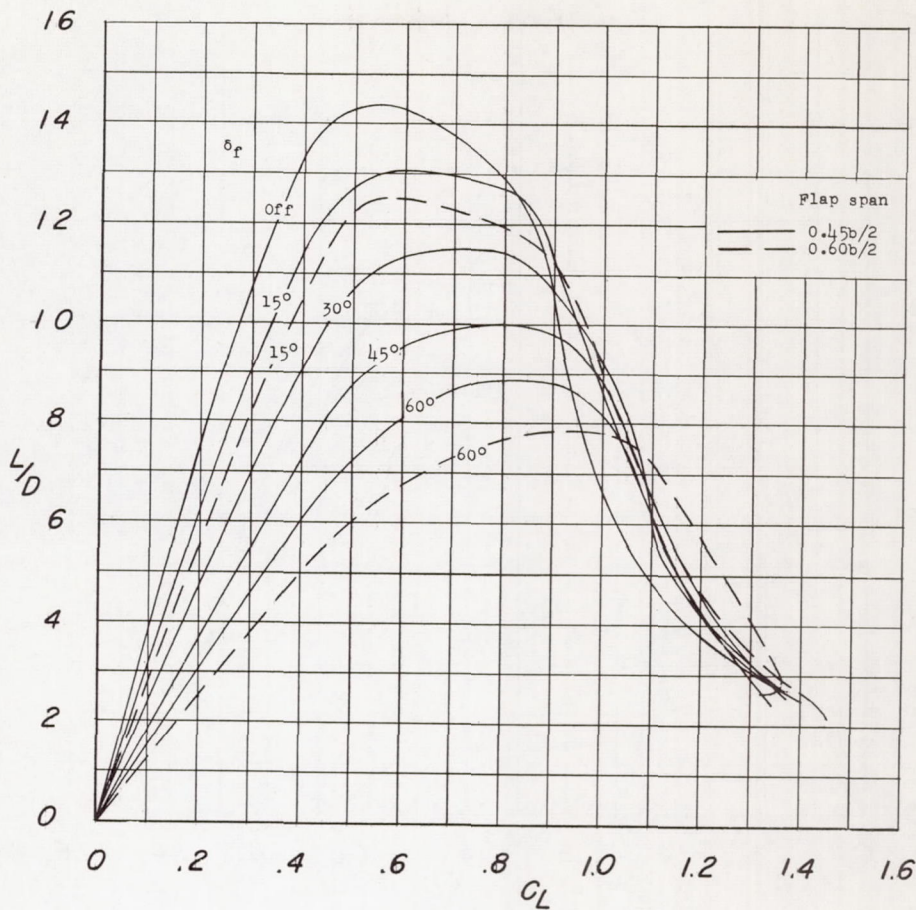
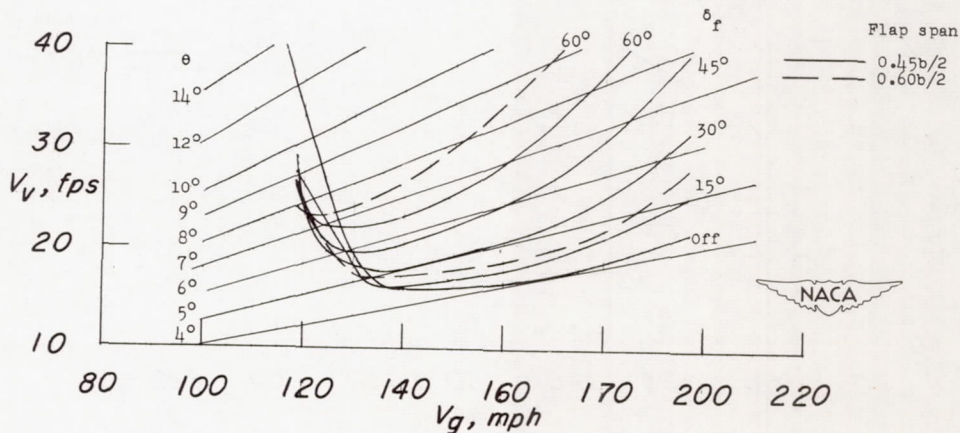


Figure 18.- Variation of the maximum lift coefficient with leading-edge-flap span for various trailing-edge flaps on the  $47.7^\circ$  sweptback-wing - fuselage combination.



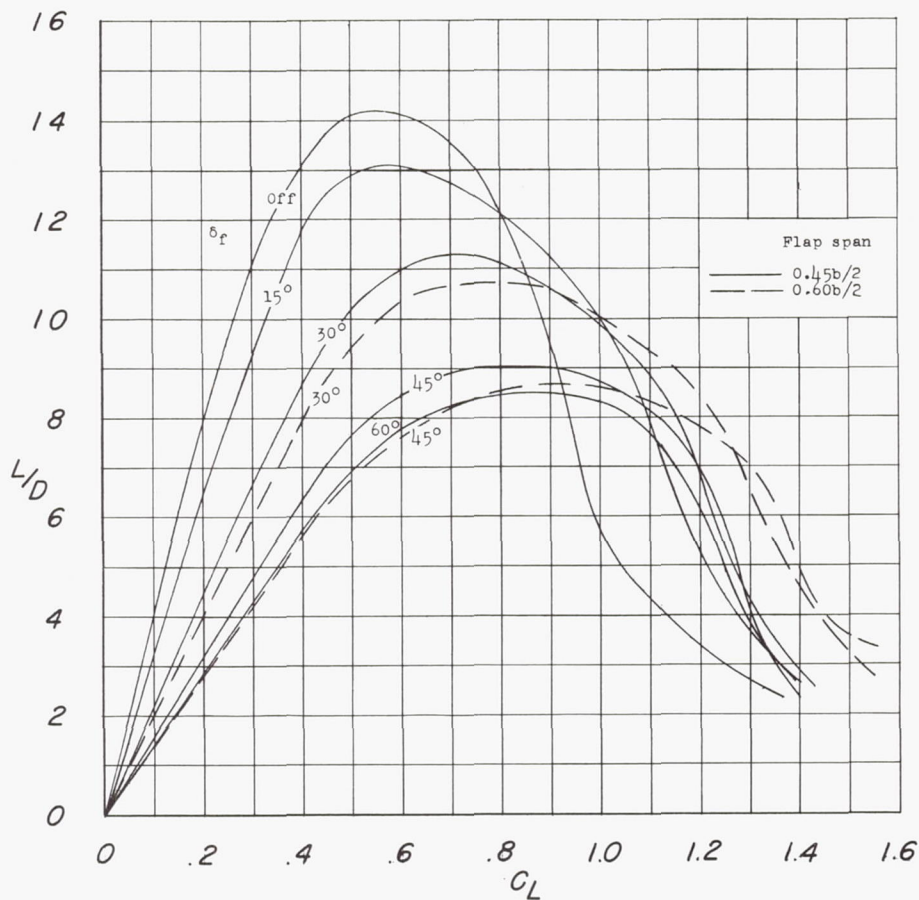


(a)  $L/D$  against  $C_L$ .

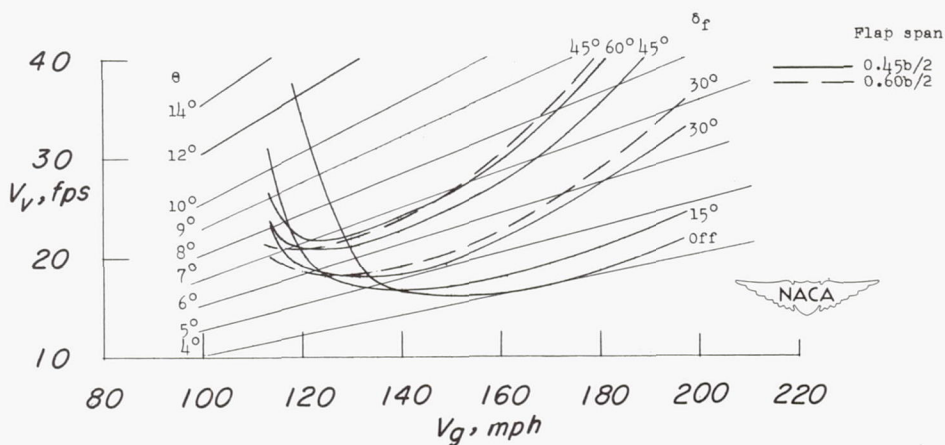


(b) Glide characteristics.

Figure 19.- Effects of split-flap deflection and span on the lift-drag ratio and the glide characteristics of the wing-fuselage combination equipped with 0.425b/2 leading-edge flaps. Assumed wing loading of 40 pounds per square foot, sea-level conditions.



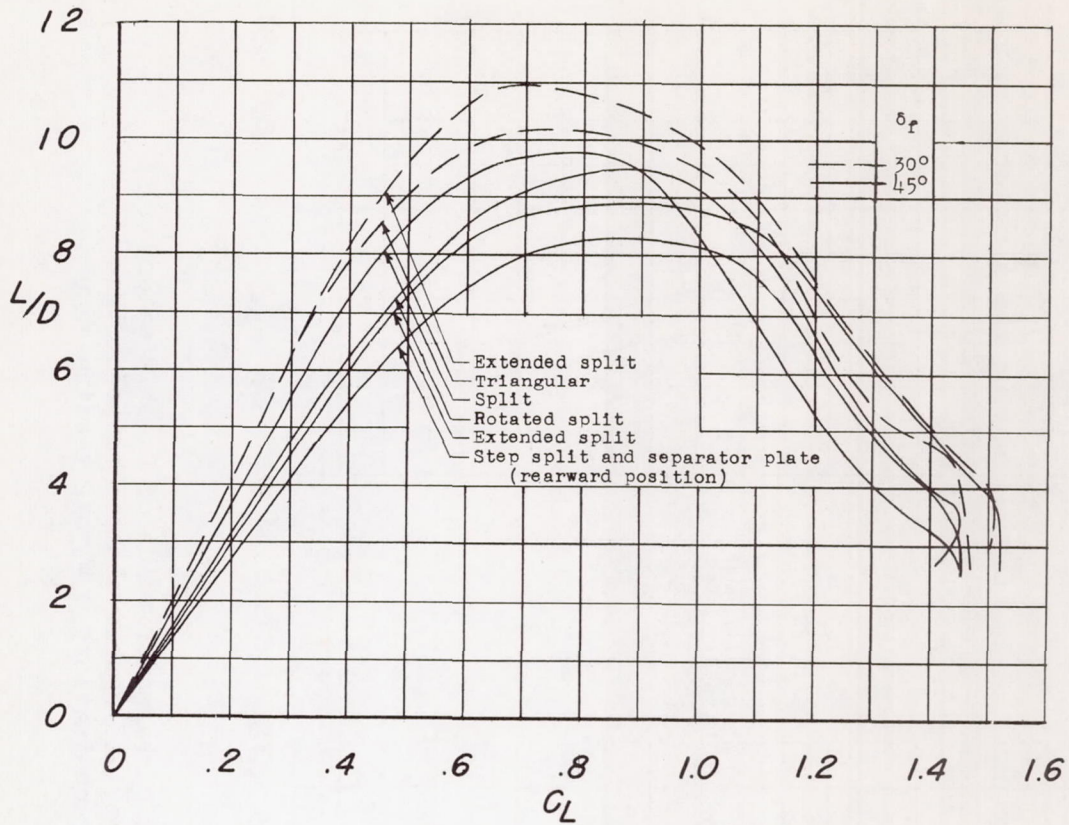
(a)  $L/D$  against  $C_L$ .



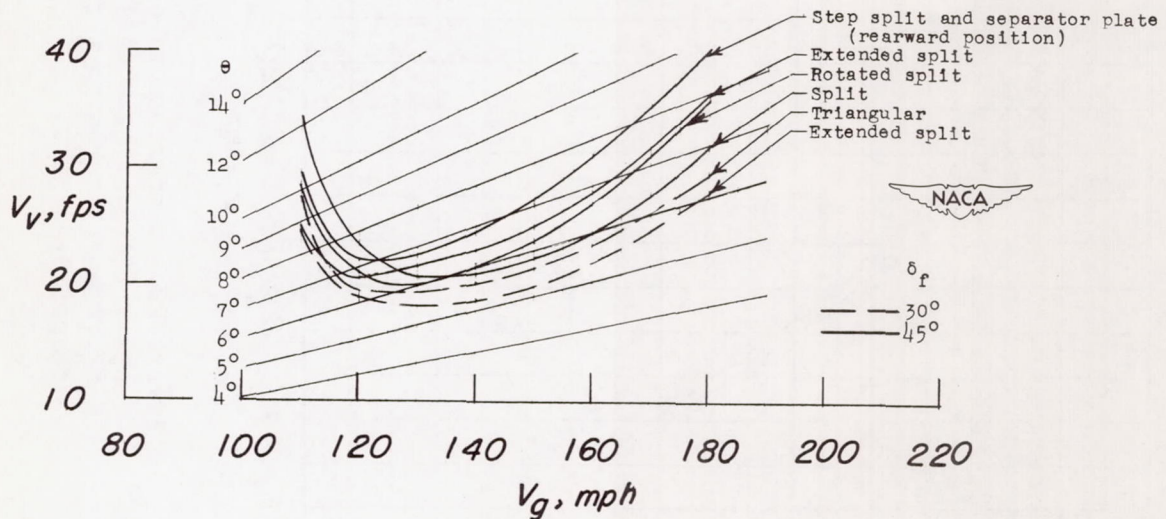
(b) Glide characteristics.

Figure 20.- Effects of extended-split-flap deflection and span on the lift-drag ratio and the glide characteristics of the wing-fuselage combination equipped with 0.375b/2 leading-edge flaps. Assumed wing loading of 40 pounds per square foot, sea-level conditions.



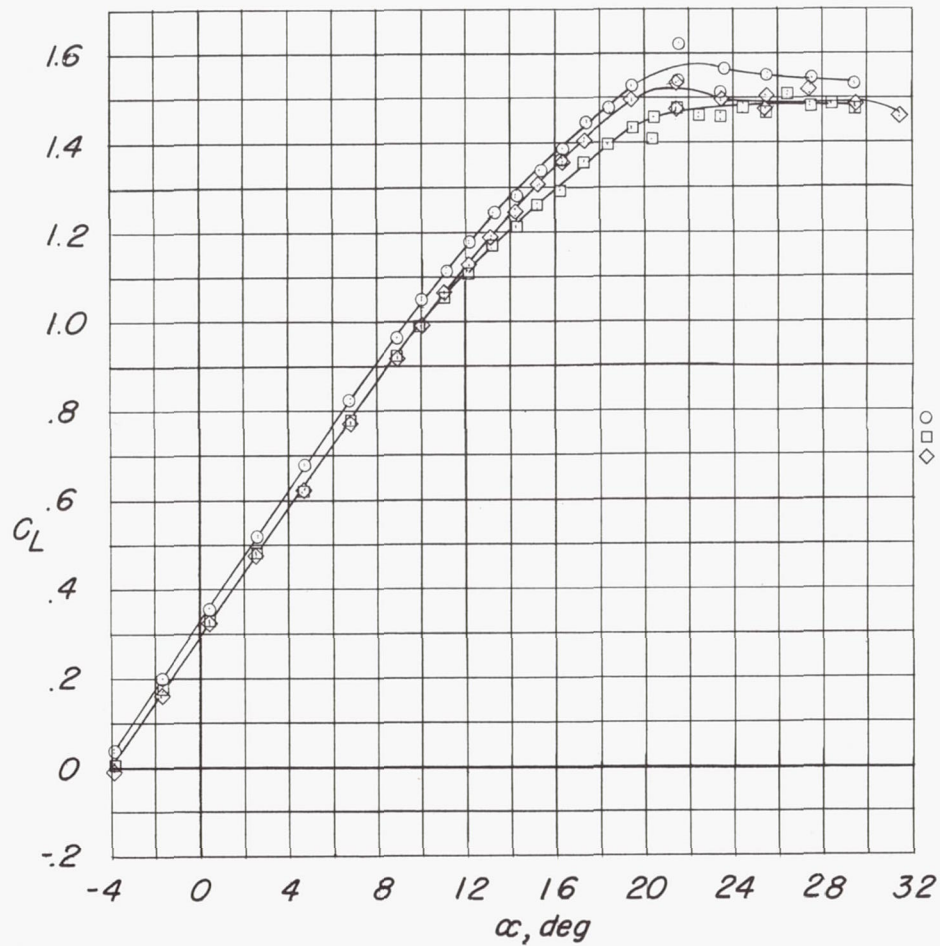


(a)  $L/D$  against  $C_L$ .



(b) Glide characteristics.

Figure 21.- Effects of various  $0.45b/2$  trailing-edge flaps on the lift-drag ratio and the glide characteristics of the wing-fuselage combination equipped with  $0.475b/2$  leading-edge flaps. Assumed wing loading of 40 pounds per square foot, sea-level conditions.



○ Double slotted  
 □ Single slotted  
 ◇ Extended split

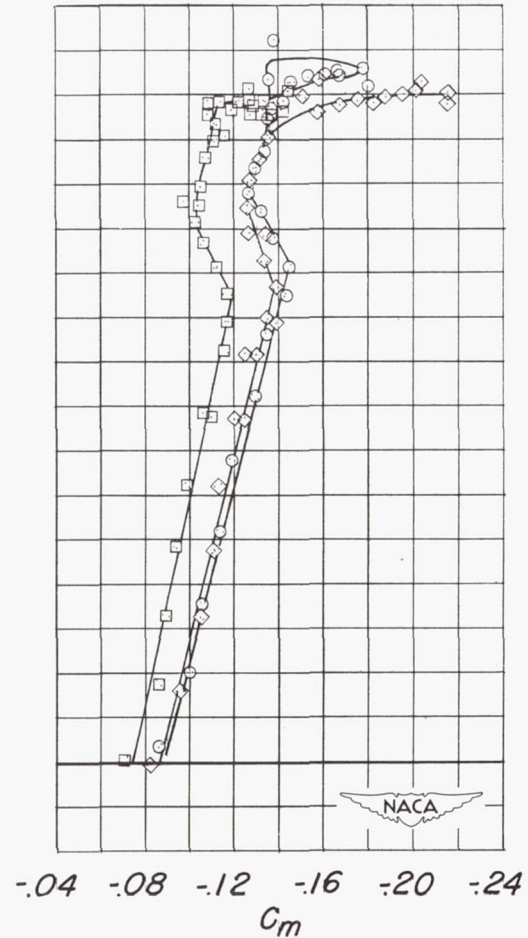
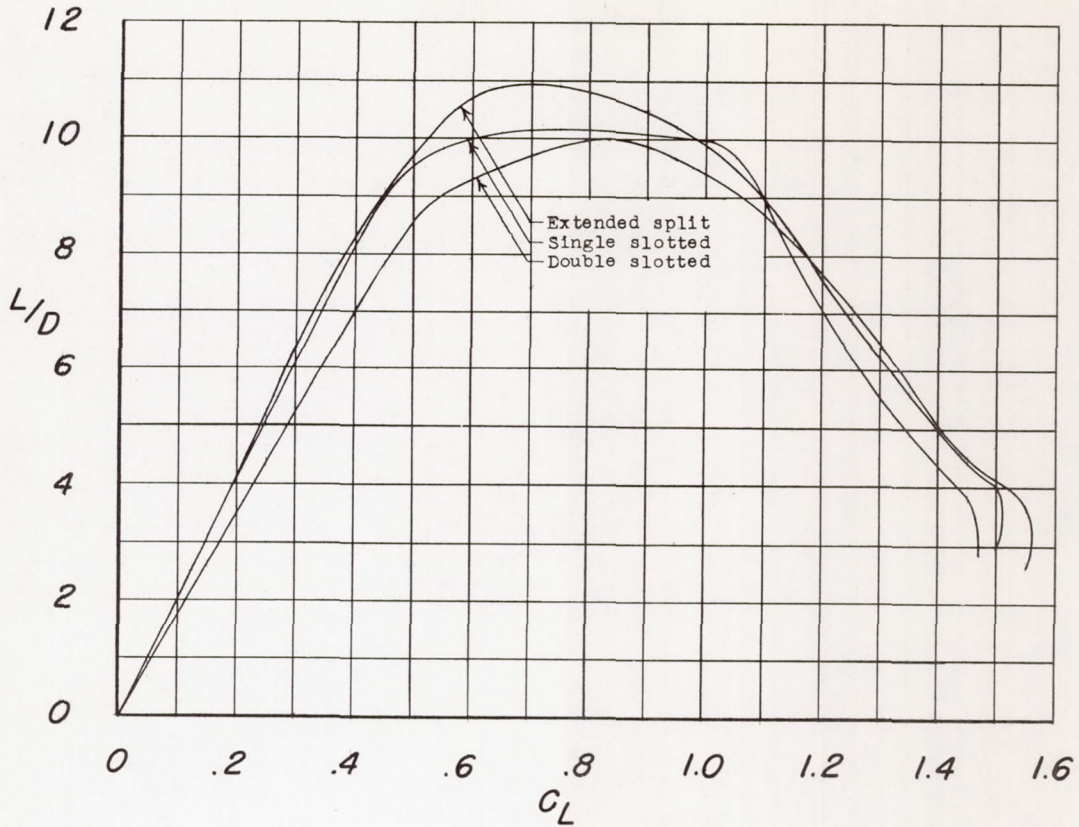
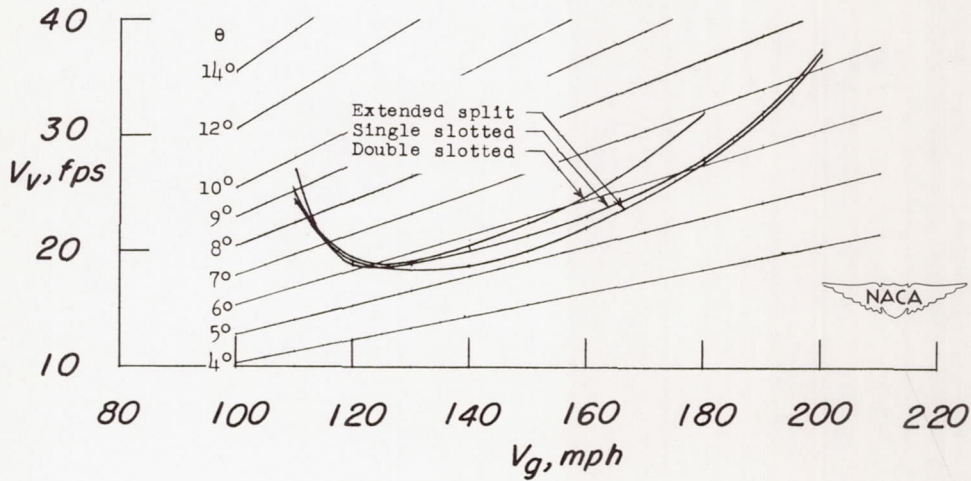


Figure 22.- Comparison of aerodynamic characteristics of 0.45b/2 extended split flaps, single slotted flaps, and double slotted flaps on the 47.7° sweptback-wing - fuselage combination; 0.475b/2 leading-edge flaps;  $\delta_f = 30^\circ$ .



(a)  $L/D$  against  $C_L$ .

(b) Glide characteristics.

Figure 23.- Effects of  $0.45b/2$  extended split, single slotted, and double slotted flaps on the lift-drag ratio and the glide characteristics of the wing-fuselage combination equipped with  $0.475b/2$  leading-edge flaps;  $\delta_f = 30^\circ$ . Assumed wing loading of 40 pounds per square foot, sea-level conditions.